ANNUAL PROGRAM REVIEW

CORROSION CONTROL

March 24, 1999

ANNUAL PROGRAM REVIEW

CORROSION CONTROL

March 24, 1999

Institute of paper Science and Technology
500, 10th Street, NW
Atlanta, GA 30318

TABLE OF CONTENTS

PROJECT F018 (RECOVERY BOILER CORROSION)

PROJECT F019 CORROSION CONTROL IN CLOSED-CYCLE MILLS

RECOVERY BOILER CORROSION

ANNUAL RESEARCH REVIEW

March 24, 1999

Preet M. Singh
Gregory J. Fonder
Safaa Al-Hassan
Sloane Stalder
Jamshad Mahmood

Institute of Paper Science and Technology
500 10th Street, N.W.
Atlanta, GA 30318

TECHNICAL PROGRAM REVIEW

Project Title:	RECOVERY BOILER CORROSION
Project Number:	F018
Division:	Chemical Recovery and Corrosion Division
Project Staff:	P. Singh, S. Al-Hassan, G. Fonder, Sloane Stalder
FY 98-99 Budget:	$31,664

Program Objectives:

Improve safety and increase operating life of equipment by proper selection of construction materials, suitable process conditions, and by understanding the possible corrosion processes in kraft recovery boilers.

Project Summary:

This section describes projects related to recovery boiler corrosion, which are funded by member dues, as well as externally funded recovery boiler projects carried out in FY-1998-99 at IPST.

Member-dues-funded project F018 is also a cost share for the bigger DOE/AF&PA project. Objectives of the F018 project were the same as those of the DOE project. The main objective of this project in FY-1998-99 was to monitor corrosive environments inside the recovery boilers that are responsible for the high corrosion rates of waterwall tubes in the lower furnace areas. The reason for that was to understand the differences in the environmental variables of a corrosive area and a non-corrosive area in the same recovery boiler. A 600-psi oscillatory gun-firing B&W boiler was chosen for this study. Three major variables affecting corrosion, i.e., temperature, chemical composition of gases, and smelt composition were monitored in the two areas. Areas for environment monitoring in this study were identified as corrosive and non-corrosive based on the yearly ultrasonic tube thickness data. Web-embedded thermocouples were used to measure the temperature differences in the two areas. On-line gas chromatography was used to analyze corrosive gases in the two areas. An attempt was also made to extract smelt from the two areas chosen. However, it was found that the monitored areas did not have any solid smelt. Therefore it can be concluded that, in these areas, smelt composition did not play any active role in the corrosion behavior of waterwall tubes. Results have indicated that the temperature difference was not responsible for the different rates of corrosion in different areas. Gas analysis has conclusively indicated that there is a significant difference in the gas composition in the two areas. Gas composition, which was in contact with the waterwall surface, was of importance from the corrosion point of view. Gases in the corrosive area had significantly higher composition of sulfur-bearing gases compared to gases in the low corrosion area. In this particular boiler, and in the chosen areas of this boiler, the difference in the gas composition was due to their firing practices, where the black liquor is sprayed on the waterwall tube surface. Due to local pyrolysis and

devolatilization reactions occurring on the surface of the tube, organo-sulfur gases and other sulfur gases, which are products of these reactions, are higher in concentration in the corrosive areas or where the spray falls on the waterwall surface.

This is the first time that such a study was carried out to explain the corrosion differences in the lower furnace areas of kraft recovery boilers. Similar work will also be carried out in other boilers with different firing practices and boiler designs. Results from the overall study, i.e., F018 and DOE/AF&PA, are described in this report.

In-situ gas analysis for kraft recovery boiler has given us a better understanding of the composition of gases that come in contact with the waterwall tubes. As a part of this project, we have started experimental work to study the kinetics of corrosion reactions in the realistic recovery boiler gas environments. Initial series of tests have been finished while other tests are continuing. This is very important information, which has not been studied in the paper industry or other industries. Knowledge of corrosive environments and their reaction kinetics is needed for prediction of material behavior as well as for the selection of appropriate materials for the lower furnace areas of kraft recovery boilers in the future. Work is also continuing to characterize the role of thermal excursions on high temperature sulfidation of carbon steels. A paper will be presented at the NACE conference and has been published by NACE as "Corrosion 99" paper # 280.

Another recovery boiler project is related to composite tube cracking in kraft recovery boilers. This project is funded at IPST by Oak Ridge National Laboratory. The objective of this project is to explore the possible stress corrosion cracking (SCC) mechanisms, which can operate during the shutdown of recovery boilers. Results from our work, ORNL investigation, and other published results indicate that composite tube cracking in kraft recovery boilers may be due to SCC. Various possible environments, including different constituents of washwater, are being studied at IPST. Slow strain rate tests were carried out to screen the possible wash water compositions and other environmental variables, which are capable of causing stress corrosion cracking of stainless steel composite tubes. Results from this study have shown that typical washwaters are capable of causing stress corrosion cracking of 304L stainless steels at temperatures between 150 & 200°C and above. Our study has indicated that the combination of NaOH and Na_2S can cause stress corrosion cracking in 304L stainless steel at temperatures as low as 50°C. Work is ongoing to understand the effect of Na_2CO_3 on stress corrosion cracking in NaOH/Na_2S mixtures. Details of this project are also included in this report for members information.

Introduction

The main objective of the projects described in this section is to understand the causes of corrosion and stress corrosion cracking of the waterwall tubes in the lower furnace of the kraft recovery boiler. Better understanding of these causes is necessary to develop successful corrosion mitigation strategies. Different types of material-related problems on the fireside have been observed and reported by various mills, and corrosion has been implicated in several smelt-water explosions over the years. Obviously, safe operation of the boiler is of prime concern, so the objective of the research program at IPST is to develop a sound understanding of the general and specific corrosion problems of kraft recovery boilers.

The focus of this program is consistent with IPST's goals for its dues-funded research program in that it is aimed at long-term implications with an emphasis on a fundamental understanding rather than a short-term quick fix without any understanding of the underlying reasons for the observed behavior. Parts of this program are leveraged with a large DOE/AF&PA project and a relatively smaller ORNL-funded project whose general objectives overlap with the overall objectives of this project.

Discussion of FY 98-99 Results

Research in the recovery boiler area, carried out at IPST in 1998-99, can be divided into two different tasks. Table I gives an overview of the structure of the overall research efforts in this area and shows how member dues-funded projects are leveraged with other externally funded projects and student research. Next to each task is a brief description of the main objective or the question that needs to be answered.

Table I. Recovery Boiler Related On-going Projects at IPST

Dues-Funded (F018)	*Additional Funding Leverage*
Monitoring of Corrosive Environment in Lower Furnace of Kraft Recovery Boiler To understand effect of different environmental variables on corrosion of waterwall tubes	DOE/AF&PA Corrosivity Monitoring of Kraft Recovery Boilers
Corrosion of Carbon Steel in Sulfur Bearing Gases To generate basic understanding kinetics of corrosion reaction in different sulfur bearing gases present in the recovery boilers	DOE/AF&PA Corrosivity Monitoring of Kraft Recovery Boilers
Externally Funded Projects	
Corrosivity Monitoring of Kraft Recovery Boilers (DOE/AF&PA)	
Stress Corrosion Cracking of Composite Tubes (ORNL)	

The report is organized to cover the status of each of the tasks shown in Table 1. The objectives and a brief summary of results from the DOE project and ORNL project on the composite tube cracking are covered at the end of this section.

Monitoring of Corrosive Environment in Lower Furnace of Kraft Recovery Boiler

Introduction

Regular inspections for the tube-wall thickness have revealed that certain areas of the waterwall in the lower furnace areas corrode at very high rates compared to the adjacent areas that do not corrode or corrode at very low rates. Corrosion in any system depends upon the material used and environmental conditions. Different materials may corrode at different rates in a given environment. However, waterwall tubes, made of the same material, show different corrosion rates in different areas of the lower furnace. Therefore, the corrosion differences in the two areas can be attributed to the differences in the environmental conditions. Previous studies have indicated that the fireside corrosion of waterwall tubes in the lower furnace is due to high temperature sulfidation. However, very little is known about the actual environments to which waterwall tubes are exposed in the lower furnace areas during recovery operation. Environment of importance to the waterwall corrosion is not the bulk environment but the local environment at/near the tube surface. This environment can be very different from the bulk environment and depends upon various factors like presence of smelt, on-wall liquor pyrolysis, other local reactions, and differences in local tube surface temperatures.

The objective of this project was to characterize local environments that come in contact with the waterwall tubes in the corrosive and the non-corrosive areas of the lower furnace of a kraft recovery boiler.

EXPERIMENTAL PROCEDURES

Selected boiler for this study was a B&W boiler, with 600 psi steam pressure. Waterwall tubes in the lower furnace were carbon steel. There were two oscillating liquor-guns in the boiler to spray black liquor for firing. The following sections briefly describe how various environmental variables were monitored in the two selected areas of this boiler. Different sampling ports installed in each area of interest are shown schematically in Figure 1.

Temperature Measurements

The main objective of temperature measurements was to monitor the differences in the waterwall temperature in the corrosive area and the non-corrosive area. Five embedded thermocouples in each area were installed in the web of the waterwall. Thermocouple tips were close to the fireside with each thermocouple at a constant distance from the fireside surface of the membrane (~3/4 way into the wall thickness). These thermocouples were fully accessible from the cold side of the boiler. Thermocouples for field study were calibrated at 4, 25, 100, and 300°C, using a standard NIST thermocouple and the data-logger which was later used at Missoula.

Gas Analysis

Gas near the waterwall tube surface was analyzed using an on-line gas chromatograph. To do so, gas-sampling ports were installed in the web of the boiler (two ports in each area of interest). Air-tight, stainless steel gas-sampling ports were welded onto the web membrane to support the ceramic tubes that were used to sample the boiler gas. Our setup was designed to eliminate any chance of leaks in the line from the area of interest to the collection point. To prevent changes in the gas composition due to high temperature corrosion of metallic gas lines, ceramic tubes were used to sample gas from these ports. Gas sampling ports are designed so that they can be accessed from the cold side of the boiler. The gas chromatographic (GC) equipment was calibrated and tested at IPST before being shipped it to the mill. Pure gases and their known mixtures were used to calibrate GC. Samples of recovery boiler gases were extracted from the areas of interest and directly injected into the GC. Gas samples were collected from, near the waterwall tube surface (behind the "smelt" and after breaking the "smelt" layer), from one inch into the boiler, and from one foot into the boiler. All samples were immediately analyzed using gas chromatographic techniques. Gas samples behind the frozen layer were very important as they reflect the environment that is in direct contact with the tube material.

Smelt Samples

Smelt-sampling ports, one ports in each selected area, were installed through the waterwall web. Smelt-sampling ports were welded onto the web membrane. Equipment required for the smelt sampling was manufactured, assembled, and tested at IPST. A specially designed ceramic spatula was used to collect the liquid smelt in the lower furnace of the recovery boiler. The "smelt" was extracted into a nitrogen-filled chamber, allowed to cool in a glove bag filled with nitrogen, and sealed in containers for later analysis in the laboratory.

Preliminary Results from Recovery Boiler Environment Monitoring

The following section provides a summary of preliminary results and a brief description of test procedures used to obtain these results at the mill.

Temperature Measurements

Boiler steam pressure was ~ 633 pounds. According to the steam tables, saturated steam temperature should be around 490°F (254.5°C). Temperature data for each thermocouple were collected every 5 minutes. Data have been collected for over three months and will be continued for at least another month. Analysis of temperature data shows that the two areas, "high corrosion" and "low corrosion", show a significant difference in thermal "spiking" (excursions). However, contrary to our expectations, there were more frequent temperature spikes in the low corrosion area, as shown in Figure 2, compared to the high corrosion area, as shown in Figure 3. If other environmental parameters are the same, temperature excursion or spiking should cause higher corrosion rates in the high temperature gaseous environments. However, we found that the temperature variation

was more in the low corrosion area than in the high corrosion area. It was also observed that the temperature spiking in the low corrosion area was related to char layer spalling from the waterwall surface, leading to a sudden rise in the local tube surface temperature. The local temperatures decreased to the steam saturation temperature as the char layer accumulated on the surface. We also observed that there was frequent activity of char accumulation and spalling in the corners of the boiler (low corrosion areas) at liquor gun level. Whereas in the corrosive area, we did not see any char buildup on the waterwall surface. This may be due to direct liquor spray on the waterwall in these areas.

Trends in the temperature data, collected over three months, have been summarized in Tables II and III. These data show that temperature excursions were more prominent in the low corrosion areas compared to the high corrosion areas, especially the temperature spikes of about 10°C or higher than the average temperature. Temperatures in the local areas will be lower as the liquid is evaporated, which in turn may prevent black liquor pyrolysis on the waterwall in this area. Lack of char buildup in high-corrosion areas may also be due to physical knocking-down of the loose char layer. In either case, the present results indicate that temperature spiking is not a determining factor for the higher corrosion rates in the corrosive area of this boiler.

Analysis of Recovery Boiler Gases

Perkin-Elmers gas chromatograph, equipped with the Thermal Conductivity Detector (TCD) and a Flame Photometric Detector (FPD), was used to analyze recovery boiler gases. Once the gas samples are injected into the chromatograph the gases in the sample are separated by specially designed columns. Light gases are detected by the TCD, whereas sulfur-bearing gases are detected by the FPD. In this document, TCD is referred to as channel A and FPD is referred to as channel B. Chromatographic equipment was calibrated using standard gases. Each gas in the sample mixture corresponds to a peak along the time axis in chromatograms. Peaks in chromatograms from the recovery boiler gas samples were identified and quantified by comparing them with our calibration gas standards. Major gaseous species identified are labeled in these chromatograms. Gas temperatures were also measured using a thermocouple through the gas-sampling port. Almost six inches inside the boiler, the gas temperature was about 900°C. However, only one inch outside from the web, inside the port, the temperature of the sample gas was less than 60°C in both areas.

1-Foot Samples

Chromatograms for the gas sample, taken from the low corrosion area with sampling tube at 1 foot inside the boiler, are shown in Figures 4 and 5. Figure 4 shows light gases from channel A and Figure 5 shows sulfur-bearing gases from channel B. These results show that the bulk gases (1 foot inside the boiler) contain N_2, H_2, CO_2, CO, CH_4, O_2, H_2S, SO_2, COS, CH_3SH, and small amounts of $(CH_3)_2S$. Actual composition of these gases is not mentioned in this report and will be provided after identifying all major peaks.

Chromatograms in Figures 6 and 7 show gas analysis for the sample taken from 1 foot inside the boiler in the high corrosion area. Comparison of Figures 4 and 6 show that the light gas composition was very similar in the two areas at 1 foot inside the boiler. Comparison of Figures 5 and 7 show that the composition of sulfur-bearing gases in these two areas are also very similar. However, there was an unidentified sulfur-bearing gas species in the high corrosion area, as shown in Figure 7. These results clearly indicate that at the depth of one foot inside the boiler, gas compositions are similar in the low corrosion and high corrosion areas of this boiler. At a depth of 1 foot, gases can be called bulk gases.

1-Inch Samples

Figures 8 and 9 show gas analysis for the gas sample taken from the low corrosion area with the sampling tube only 1 inch inside the boiler. It was noted that the light gas concentrations, relative to the 1-foot gas sample from the low corrosion area shown in Figure 4, decreased for CO, O_2, and N_2, whereas concentrations of H_2, CH_4, and CO_2 increased, as shown in Figure 8. In the low corrosion area, the concentration of sulfur gases was slightly higher at 1 inch compared to that at 1 foot. Chromatograms for the 1-inch gas sample from the high corrosion areas are shown in Figures 10 and 11. Comparison of Figure 11 with Figure 7 shows that the sulfur-bearing gases, notably H_2S, COS/SO_2, and CH_3SH, were higher in the 1-inch samples relative to samples from 1 foot inside the boiler. The initial portion of chromatogram, for about five minutes, is very busy with broadened peaks, where the concentrations of H_2S and COS/SO_2 are above the detection limits of the chromatograph detector, resulting in peak broadening along the time axis and peak overlap in this region. An increase in the amount of $(CH_3)_2S$, as well as the appearance of CS_2, was detected for the 1-inch samples taken from both areas of the boiler.

Flush Samples

Gas that comes in contact with the waterwall was collected and analyzed by keeping the ceramic tube tip flush with the waterwall surface. Figures 12 and 13 show chromatograms for the "flush sample" from the low corrosion area. Chromatograms in Figures 14 to 17 are for the flush samples from the high corrosion area. It is clear from these results that the composition of gas which comes in contact with the waterwall is significantly different in the high corrosion area compared to the low corrosion area. Numerous sulfur- bearing species, which were not found in bulk gases, were found in the flush sample for the high as well as low corrosion areas. Figures 18 to 22 show average concentration of different sulfur gases and other major light gases in the two areas. These results clearly indicate that the sulfur-bearing gases were always higher in the samples taken from the high corrosion areas, near the waterwall surface, compared to the equivalent samples taken from the low corrosion area. Concentration of sulfur-bearing species dropped significantly in the samples taken from 1 foot away from the waterwall surface, which can be considered to be diluted and similar to the bulk recovery boiler gases in this region. However, the waterwall surface in a high corrosion area comes in contact with the higher concentrations

of sulfur-bearing gases than in low corrosion areas, where black liquor does not fall on the waterwall surface. Concentrations of sulfur-bearing gases were significantly higher in the high corrosion areas. Hot unburned black liquor as well as pyrolysis of black liquor at the waterwall, close to the sampling tube, releases sulfur-bearing gases in the high corrosion area. This results in higher local concentrations of H_2S and organo-sulfur gases (methyl mercaptans, dimethyl sulfide, carbonyl sulfide), which further leads to higher corrosion in the local areas. Our laboratory results show that at 400°C, SA-210 samples corrode at ~50 mpy in 1% CH_3SH (methyl mercaptan) compared to ~5 mpy in 1% H_2S. At 320°C, corrosion rates were ~6 mpy in a 1% methyl mercaptan test compared to ~1 mpy in a 1% H_2S gas mix.

Tests for Chlorine Bearing Gases

Recovery boiler gases were collected in two glass gas collection vessels, with deionized ultra-filtered water, connected in series. Flow rates and collection times of gas were noted. Samples of water through which gas had been bubbled were sealed in vials for analysis at IPST. Samples from all 6 sampling conditions were analyzed using capillary ion electrophoresis. When compared against a chloride standard, all six samples were deemed to have no chlorides present. This result, however, does not prove that there is no chloride present in the recovery boiler gases. It only proves that there was no chloride in the gas by the time it reached the gas collection vessels. Condensation of chloride species or entrapment of possibly generated HCl in condensed water could have prevented any detectable chloride from reaching the vessels. However, chlorides are not suspected to be involved in the corrosion mechanisms operating in the lower furnace of this recovery boiler.

Smelt samples

The "smelt" was extracted in a nitrogen-filled chamber, allowed to cool in a glove bag filled with nitrogen, and sealed in airtight containers for further lab analysis. We did not find any flowing smelt in either of the areas monitored. In each sampling, the ceramic spatula was filled with unburnt-char and not the smelt. After several trials we did not see any signs of thick frozen smelt in either area. The char deposits accumulate on the waterwall surface in the form of a loose, porous layer that is a good insulator. This layer spalls frequently and is replaced by a new layer in a very short period. We found a correlation between the char-layer spalling and temperature excursions in the local area.

CONCLUSIONS AND PRACTICAL IMPLICATIONS

Local concentrations of organo-sulfur gases, in general, and methyl mercaptan, in-particular, explain higher local corrosion rates in the local area where liquor is sprayed on the waterwall. Based on our results, we can conclude that as the black liquor is deliberately sprayed on the sidewalls using oscillatory liquor guns, the local gaseous composition in this "butterfly area" is rich in sulfur gas products due to black liquor heating and pyrolysis. As liquor is sprayed directly on the sidewalls, the local temperatures in the corrosive area may not reach a value required for pyrolysis reaction to occur. This was evident from the fact that clear liquid, probably from the black liquor, was occasionally found in gas sampling ports in the corrosive area. In this area, char does not build on the surface. We did not find any signs of frozen or flowing smelt in the corrosive area. Char buildup in the high corrosion area is far less than in the corner of the boiler where corrosion rates are very low.

Based on our results from the environment monitoring work done at Missoula, the following conclusions can be drawn:

1. Temperature differences or temperature fluctuation do not have a significant influence on the difference in the corrosion rates of waterwall tubes in the two selected areas.

2. Frozen smelt was found on the waterwall surface of the selected areas at the liquor gun level, therefore, differences in smelt compositions do not affect corrosion in the two areas. However, char layer buildup in the two areas is different. Char layer buildup is more prominent in the low corrosion area, in the corner of the boiler, than in the corrosive area, where liquor is sprayed on the walls. Char layer spalling causes sudden temperature spikes, detected in the corner of this boiler, in the low corrosion area.

3. Gas compositions on the waterwall surface in the two selected areas are significantly different. High concentrations of sulfur-bearing gases were detected in the corrosive area compared to the low corrosion area.

4. High concentrations of organo-sulfur gases in the corrosive areas are due to direct spraying of black liquor on the waterwalls in this area. The sulfur species are available in the local area to react with the metal surface to sulfidize it and cause higher rates of corrosion in the local areas only.

5. These results and our other laboratory work suggest that higher rates of corrosion in the local areas can be controlled by avoiding direct spraying of black liquor on the waterwall surface.

6. These conclusions are for the monitored areas only. Other reasons/variables may be important in other parts of a given boiler and should be monitored while considering those areas.

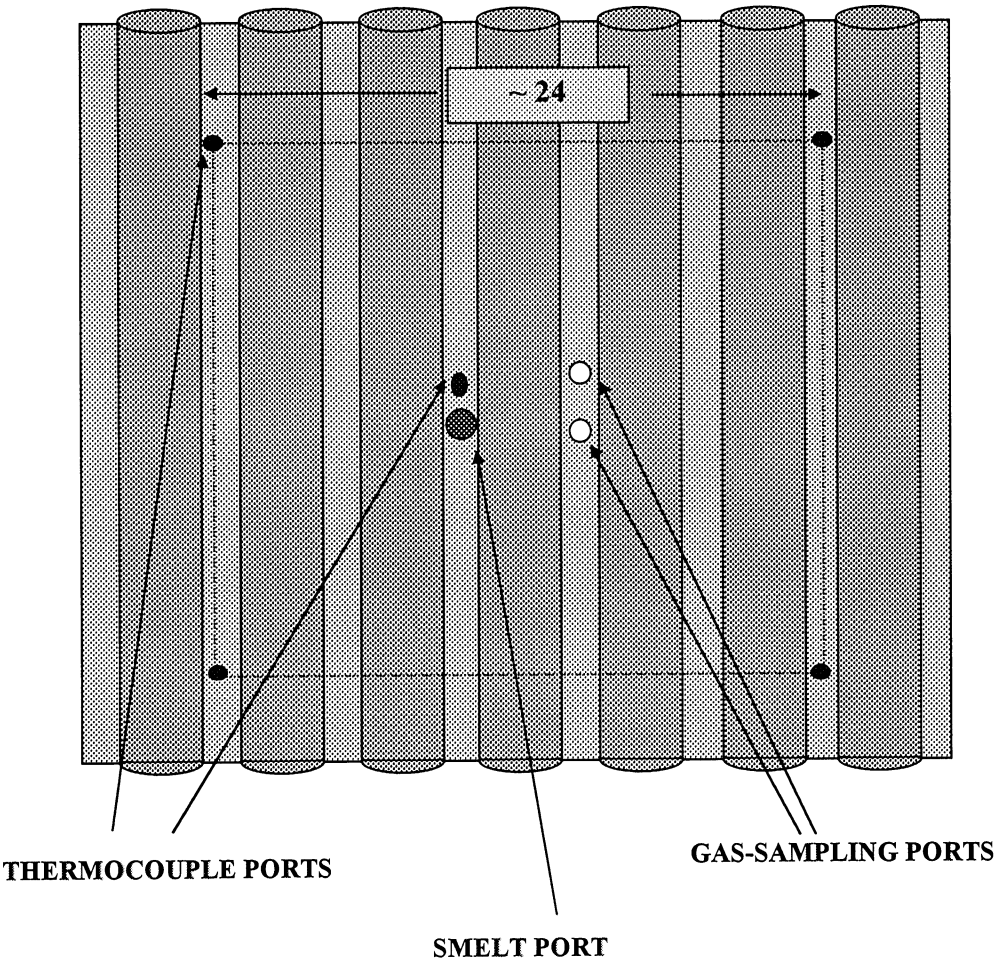

Figure 1. Schematic showing general arrangement of sampling ports installed in the corrosive and low-corrosion areas of the recovery boiler furnace. Five thermocouples were installed in each area.

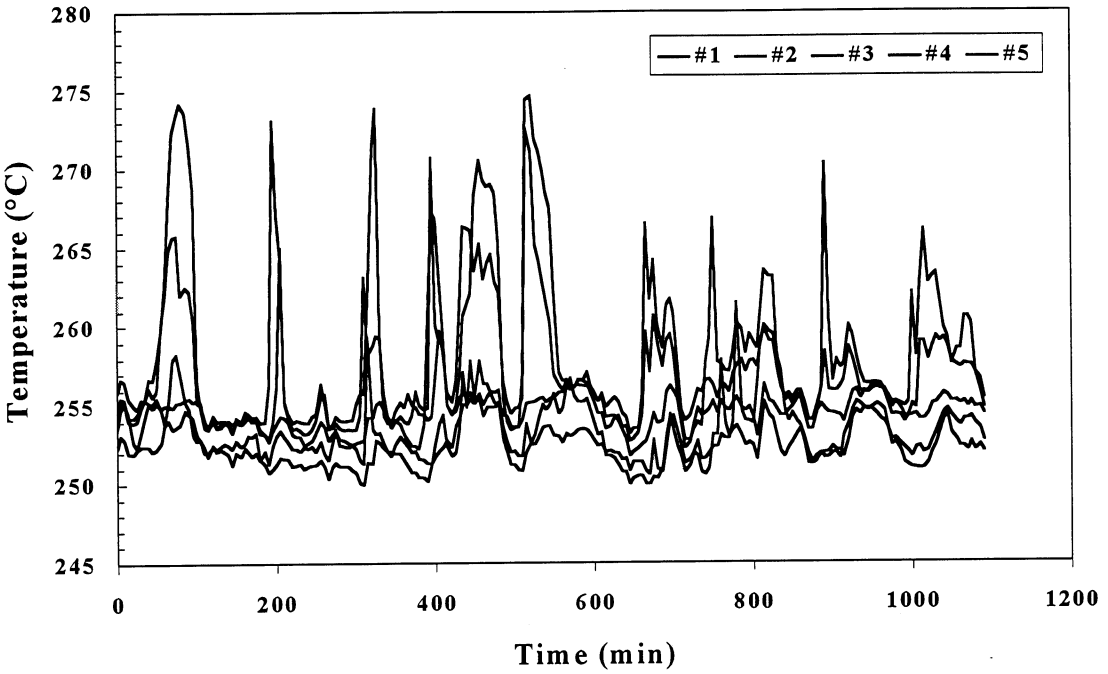

Figure 2. Waterwall temperature data from five thermocouples installed in the "low corrosion" area of the recovery boiler.

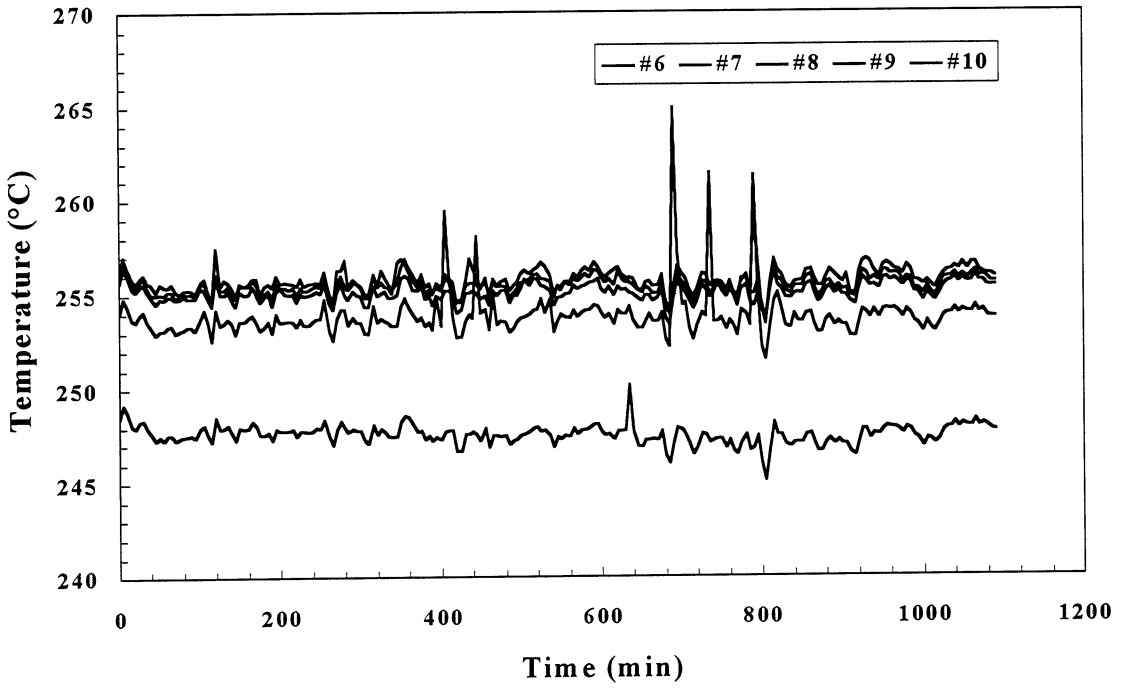

Figure 3. Waterwall temperature data from five thermocouples installed in the "corrosive area" of the recovery boiler furnace.

Table II. Summary of temperature spikes detected at different locations over a period of three months.

	Spikes above 10°C	Spikes above 15°C	Spikes above 20°C	Spikes above 25°C
TC #1 (Low Corr.)	243	108	18	0
TC #2 (Low Corr.)	58	25	13	2
TC #3 (Low Corr.)	194	58	11	1
TC #4 (Low Corr.)	109	21	0	0
TC #5 (Low Corr.)	154	52	4	0
TC #6 (High Corr.)	637	461	133	30
TC #7 (High Corr.)	494	114	34	5
TC #8 (High Corr.)	783	462	145	38
TC #9 (High Corr.)	1201	674	401	114
TC #10 (High Corr.)	735	516	230	71

Table III. Statistics of temperature data for each location collected over three months.

	TC #1	TC #2	TC #3	TC #4	TC #5	TC #6	TC #7	TC #8	TC #9	TC #10
Max. Temperature	278.75	280.85	285.92	275.82	282.76	285.94	273.86	290.52	295.24	296.79
Min. Temperature	233.27	233.52	235.87	235.04	236.53	237.83	231.91	239.19	239.34	239.67
Avg. Temperature	255.46	255.19	259.65	256.89	258.97	254.56	248.12	256.26	257.28	256.54
Temperature Range	45.48	47.33	50.05	40.78	46.23	48.11	41.95	51.33	55.90	57.12
Standard Deviation	3.07	2.36	3.11	2.17	3.01	3.01	2.23	3.31	4.24	3.35

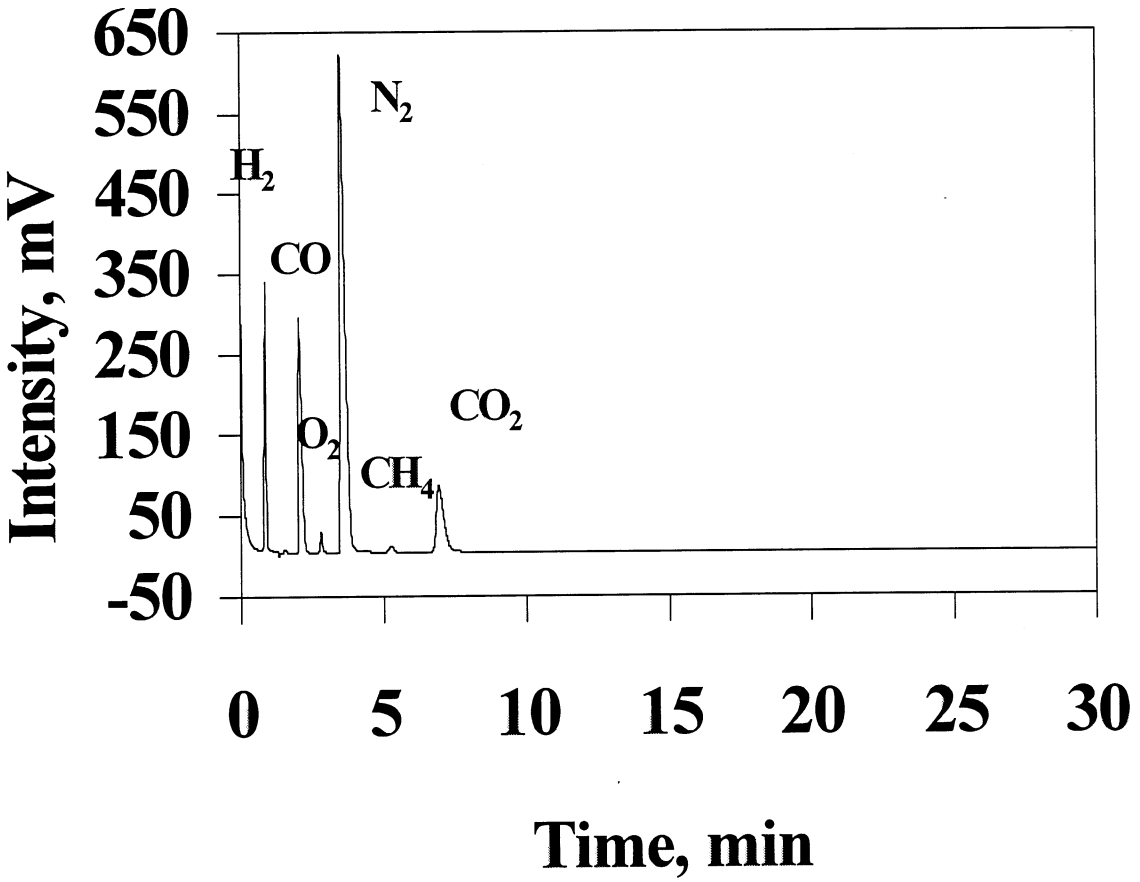

Figure 4. Chromatogram showing light gases for a sample taken from 1 foot inside the boiler in the "low corrosion area."

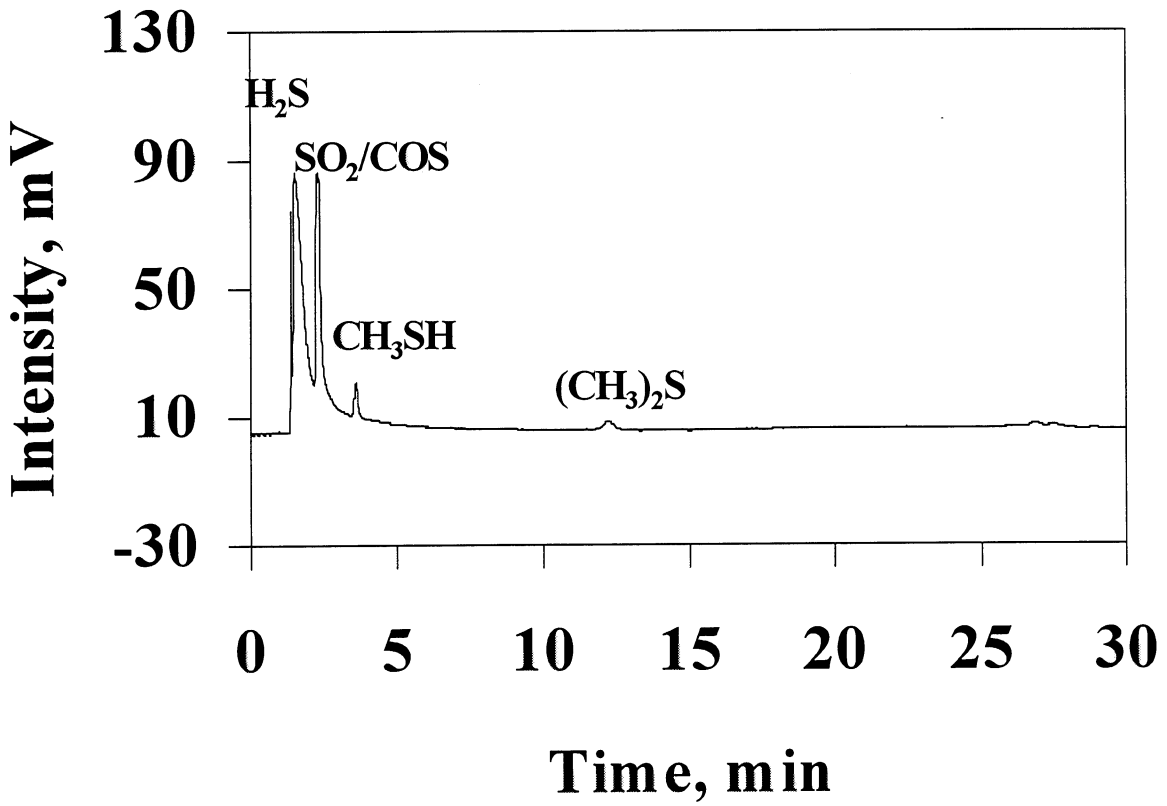

Figure 5. Chromatogram showing sulfur-bearing gases for a sample taken from 1 foot inside the boiler in the "low corrosion area."

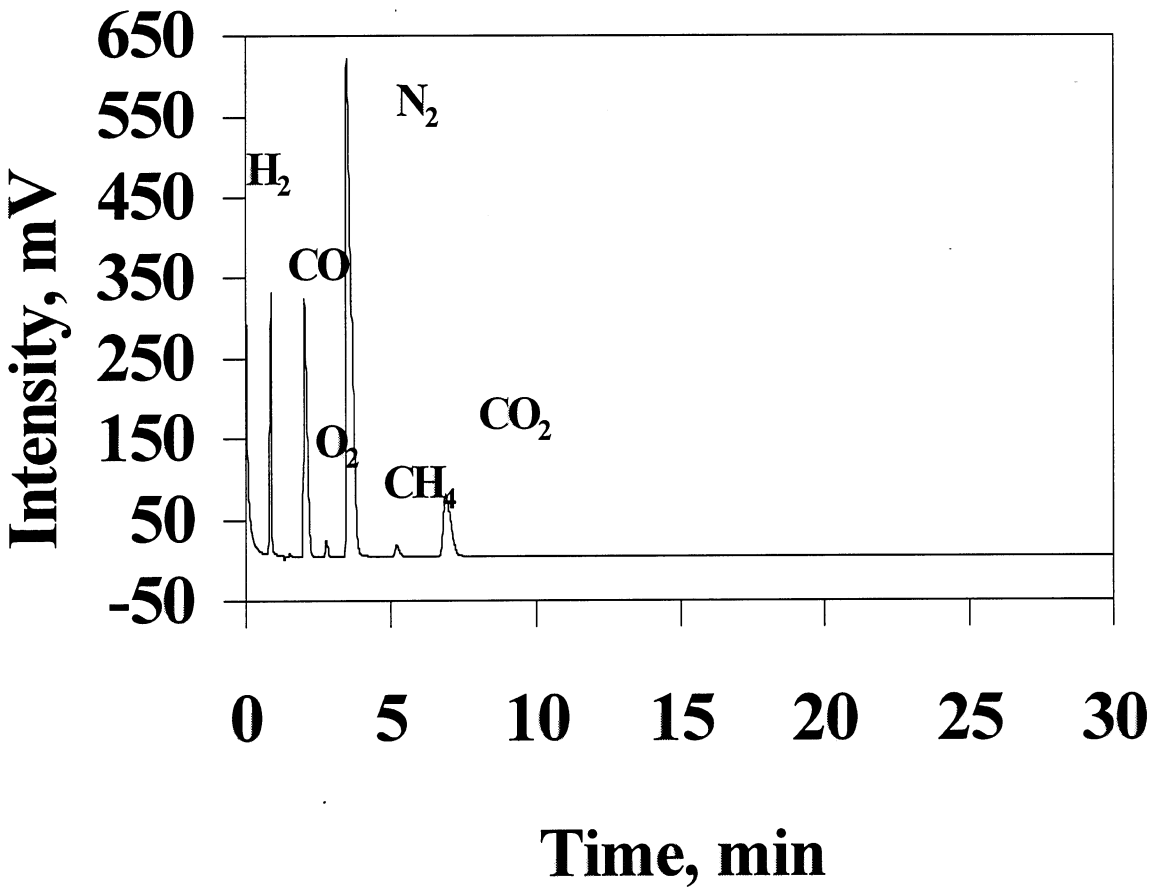

Figure 6. Chromatogram showing light gases for a sample taken from 1 foot inside the boiler in the "corrosive area."

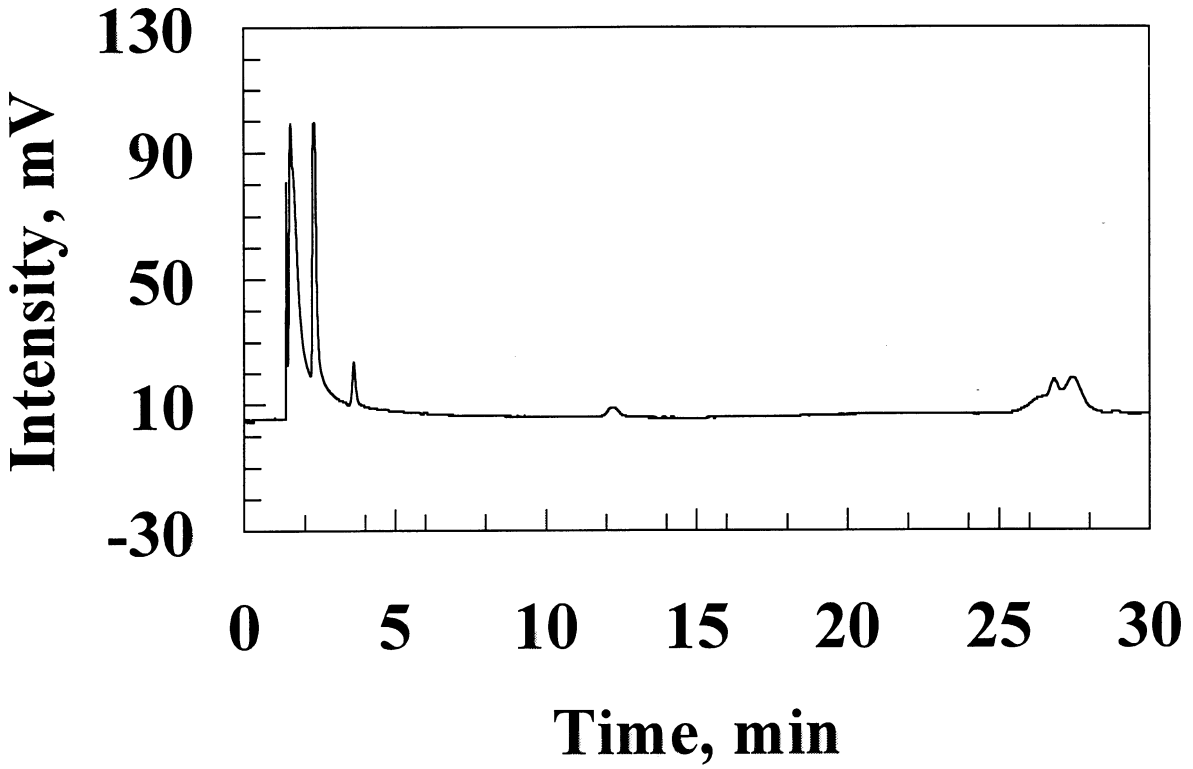

Figure 7. Chromatogram showing sulfur-bearing gases for a sample taken from 1 foot inside the boiler in the "corrosive area."

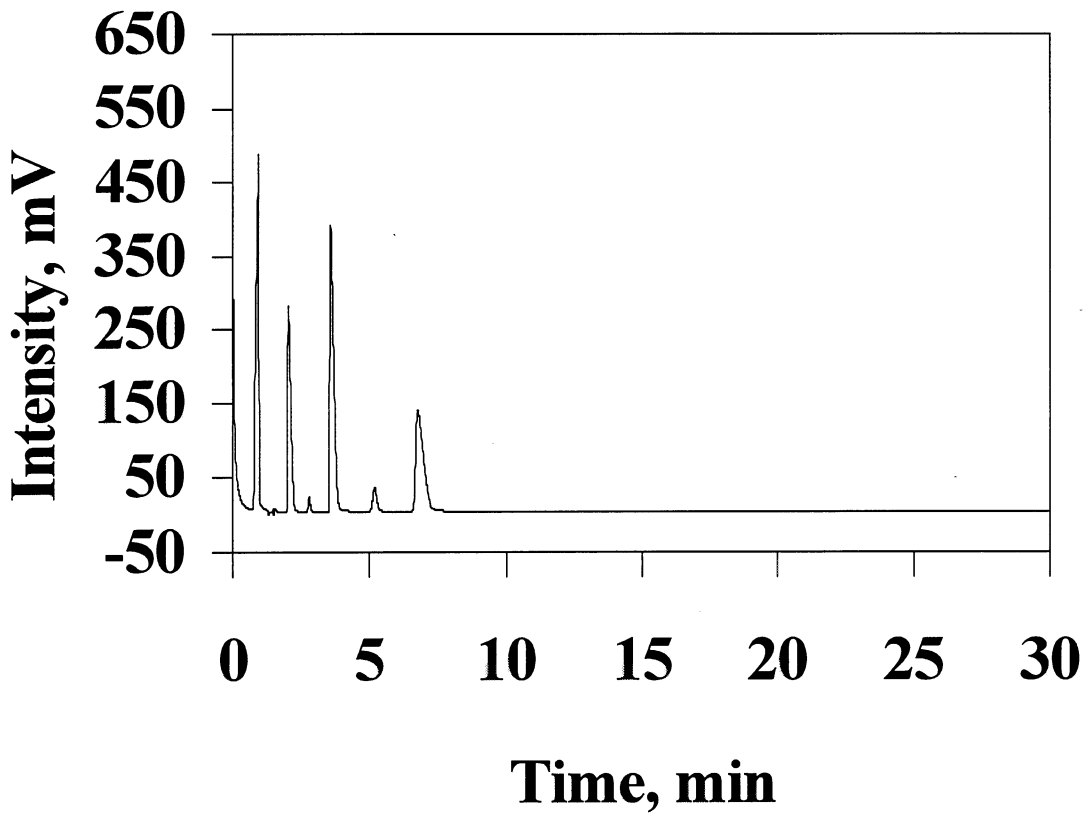

Figure 8. Chromatogram showing light gases for a sample taken from 1 inch inside the boiler in the "low corrosion area."

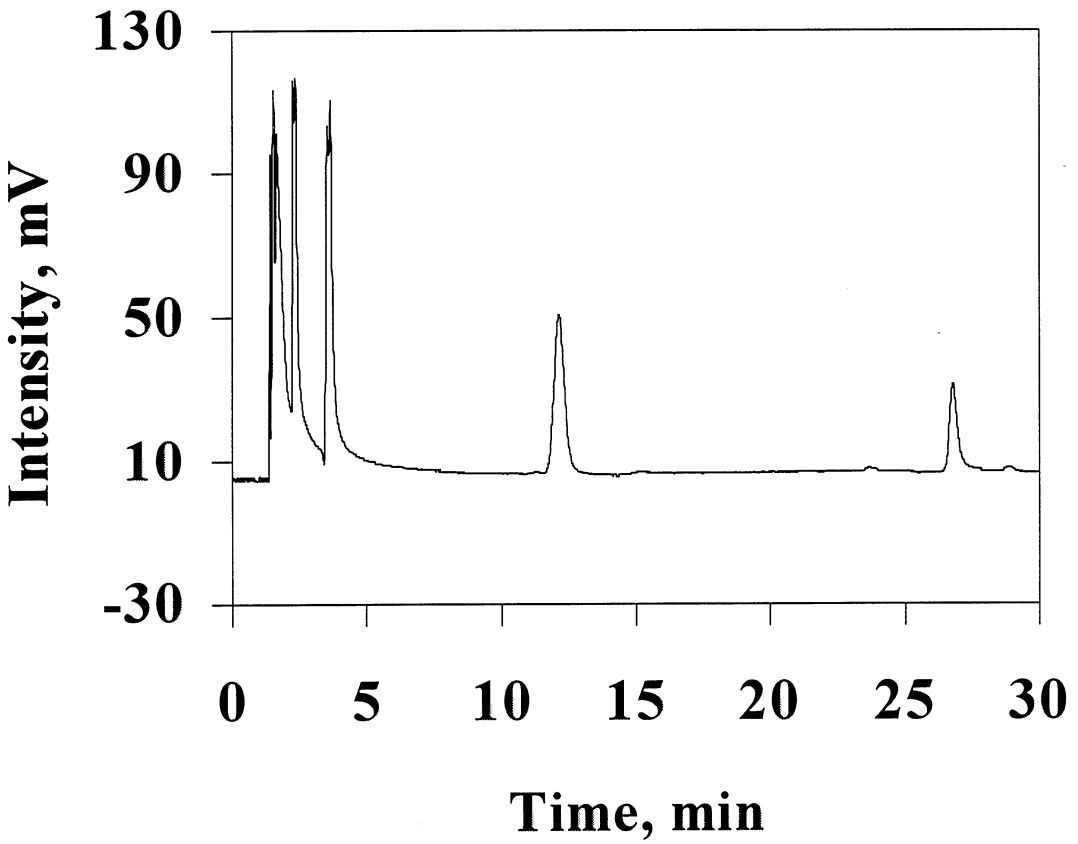

Figure 9. Chromatogram showing sulfur-bearing gases for a sample taken from 1 inch inside the boiler in the "low corrosion area."

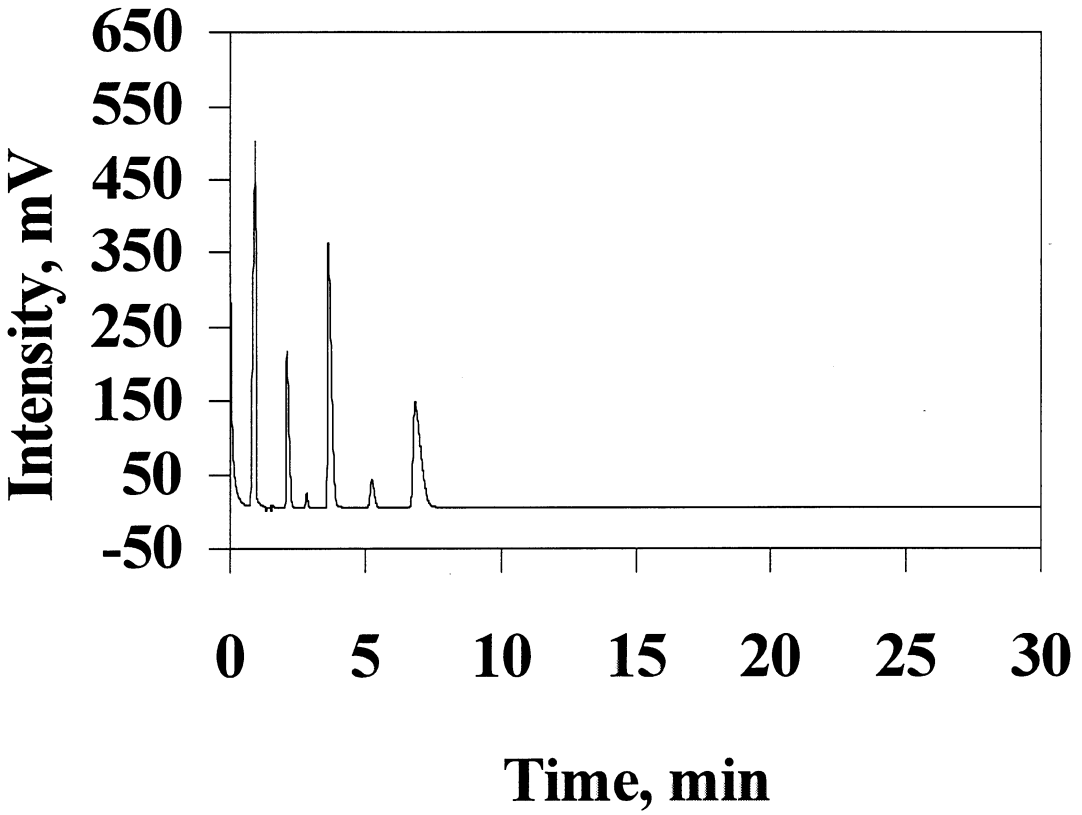

Figure 10. Chromatogram showing light gases for a sample taken from 1 inch inside the boiler in the "corrosive area."

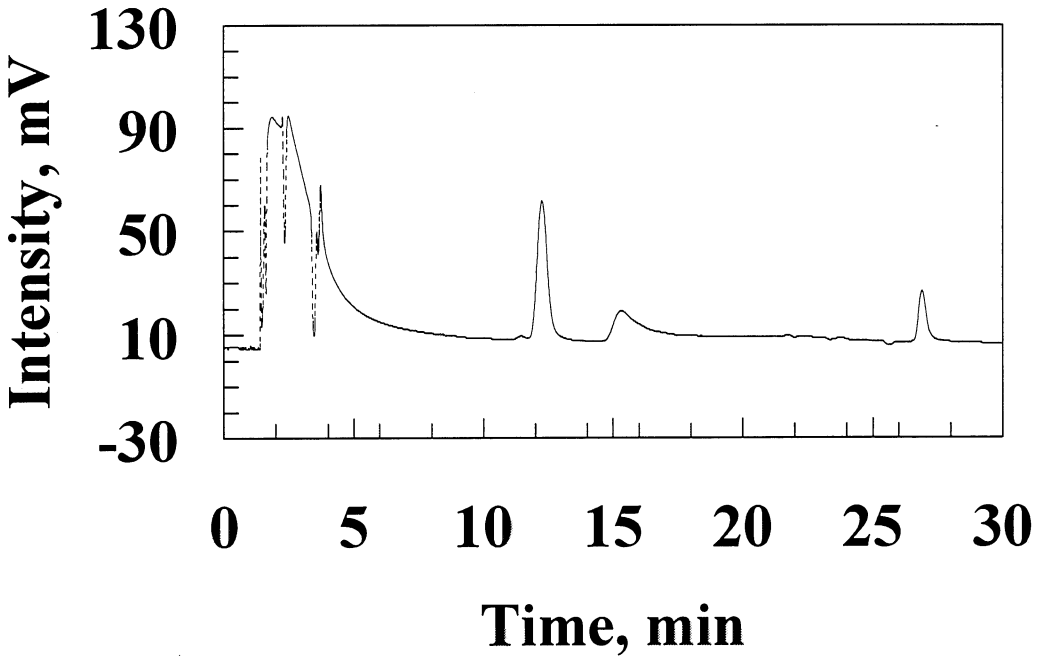

Figure 11. Chromatogram showing sulfur-bearing gases for a sample taken from 1 inch inside the boiler in the "corrosive area."

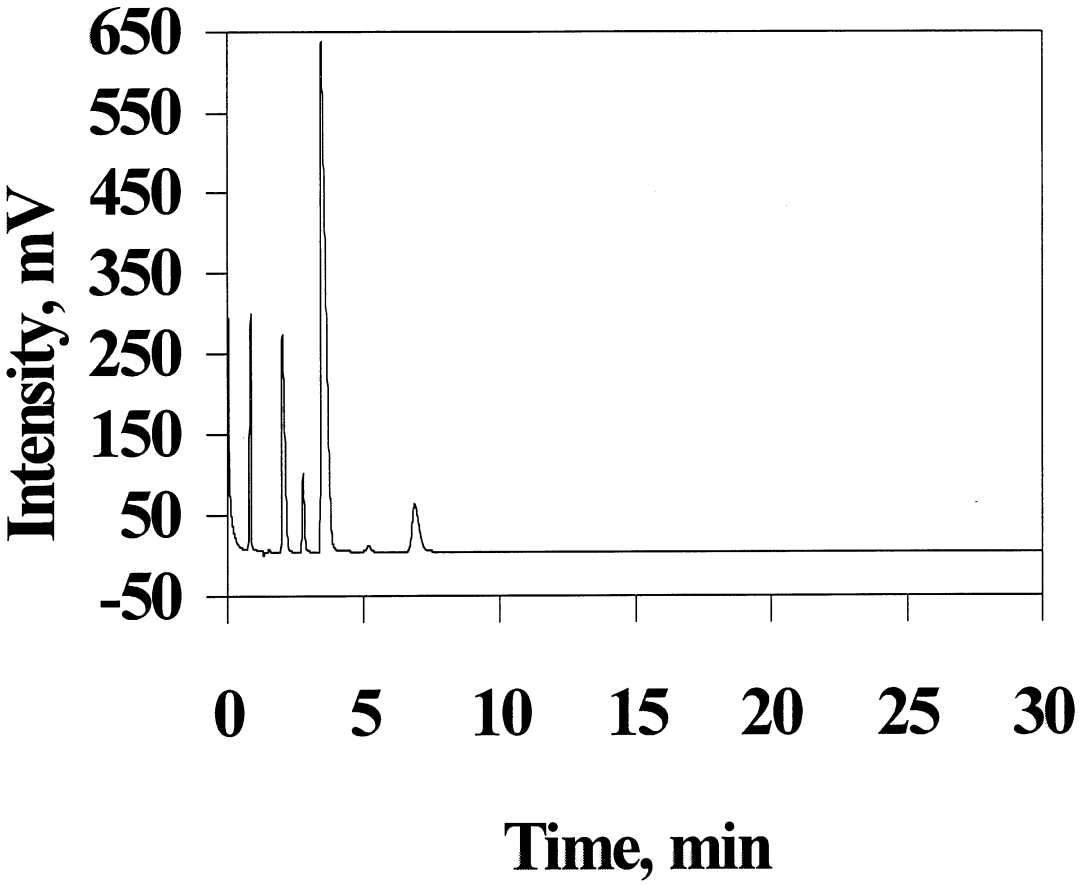

Figure 12. Chromatogram showing light gases for a sample taken with tube flush with waterwall surface inside the boiler in the "low corrosion area."

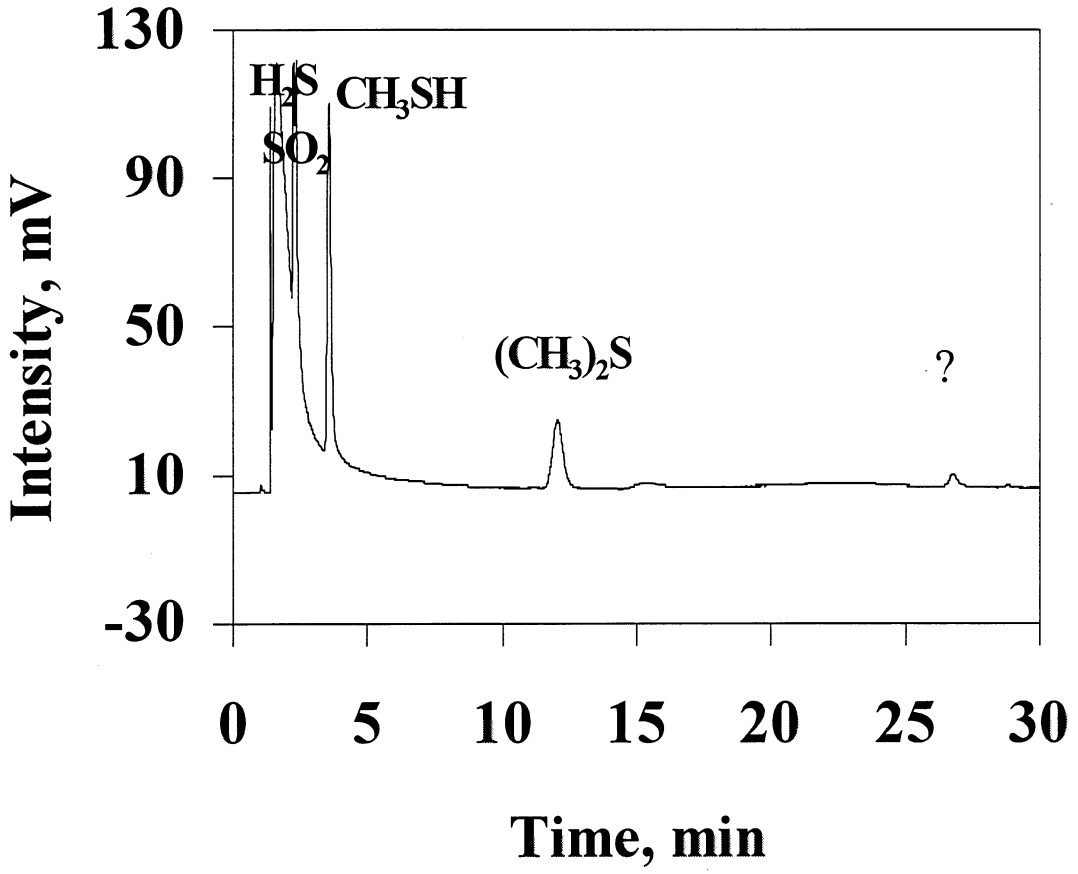

Figure 13. Chromatogram showing sulfur-bearing gases for a sample taken with tube flush with waterwall surface inside the boiler in the "low corrosion area."

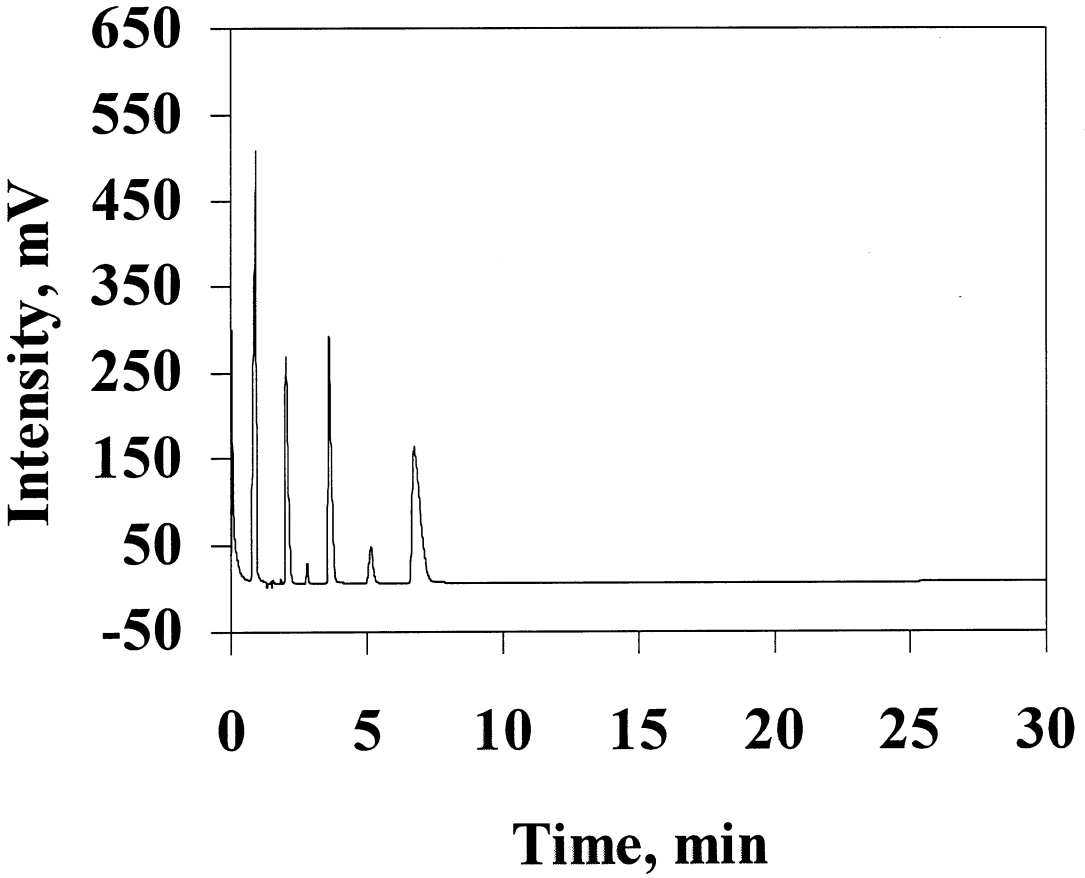

Figure 14. Chromatogram showing light gases for a sample taken with tube flush with waterwall surface inside the boiler in the "corrosive area."

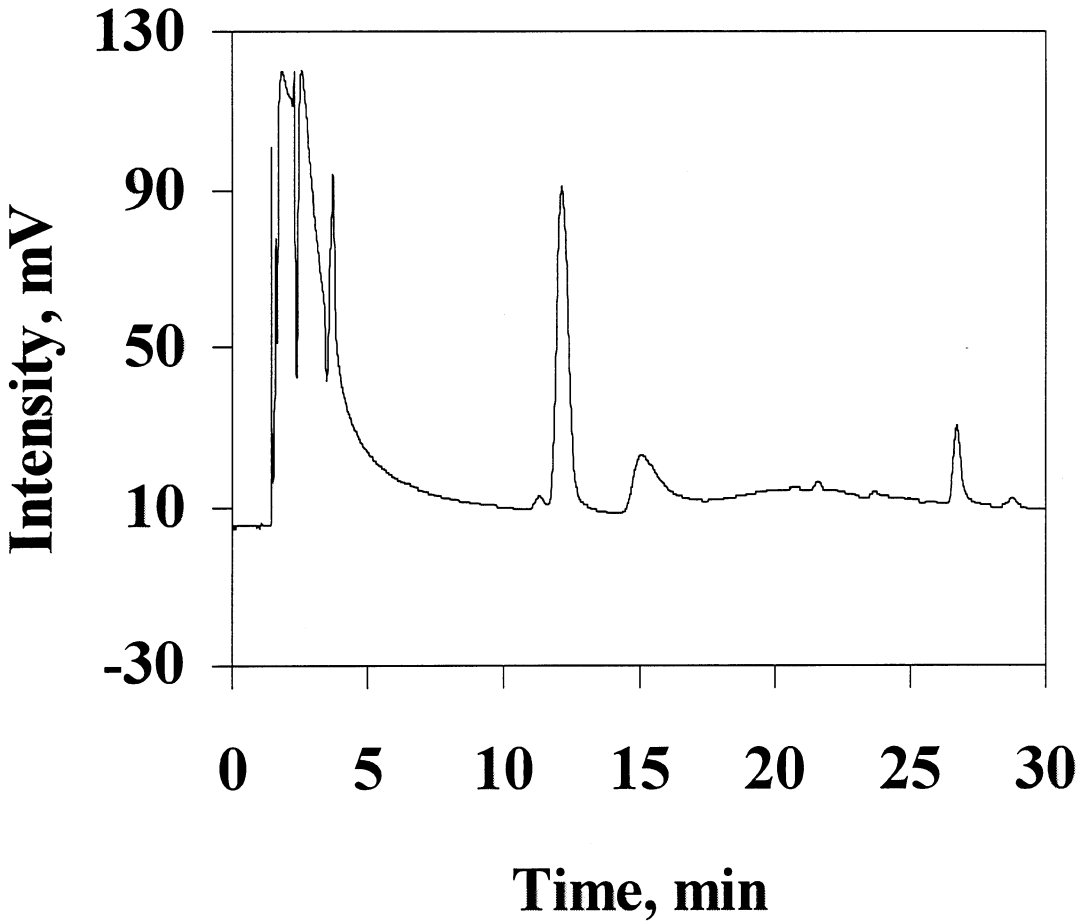

Figure 15. Chromatogram showing sulfur-bearing gases for a sample taken with tube flush with waterwall surface inside the boiler in the "corrosive area."

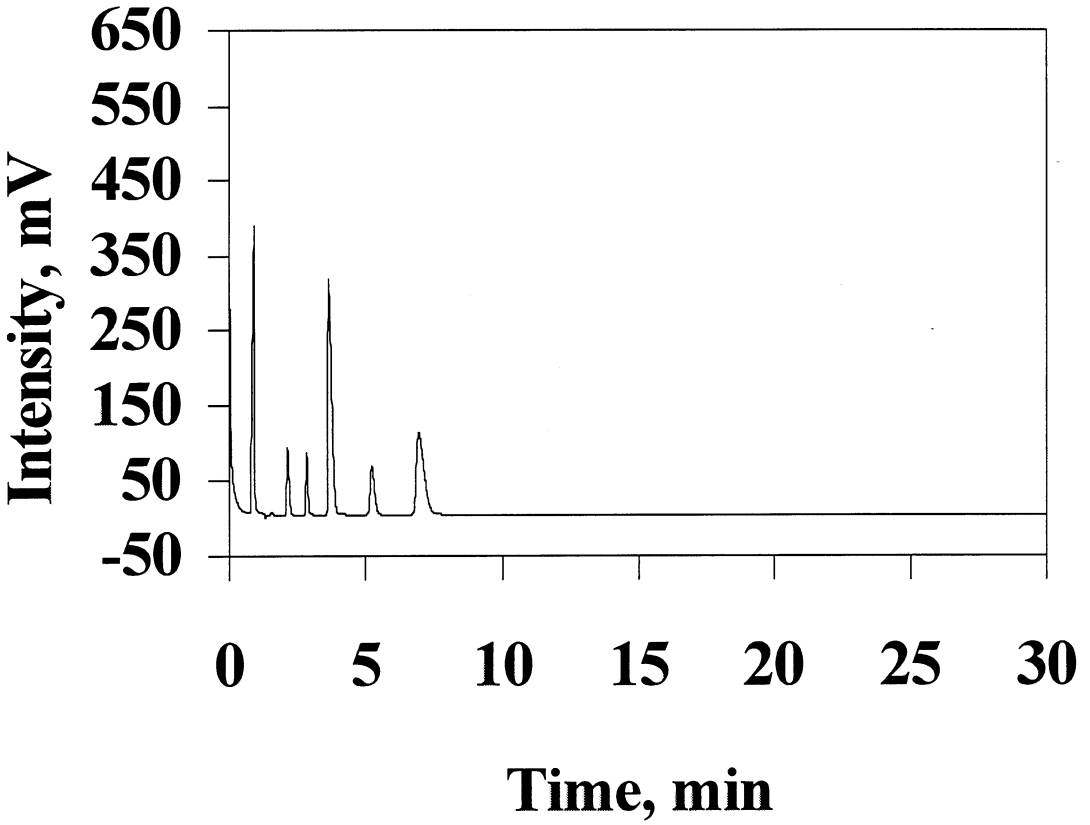

Figure 16. Chromatogram showing light gases for a sample taken with tube flush with waterwall surface inside the boiler in the "corrosive area."

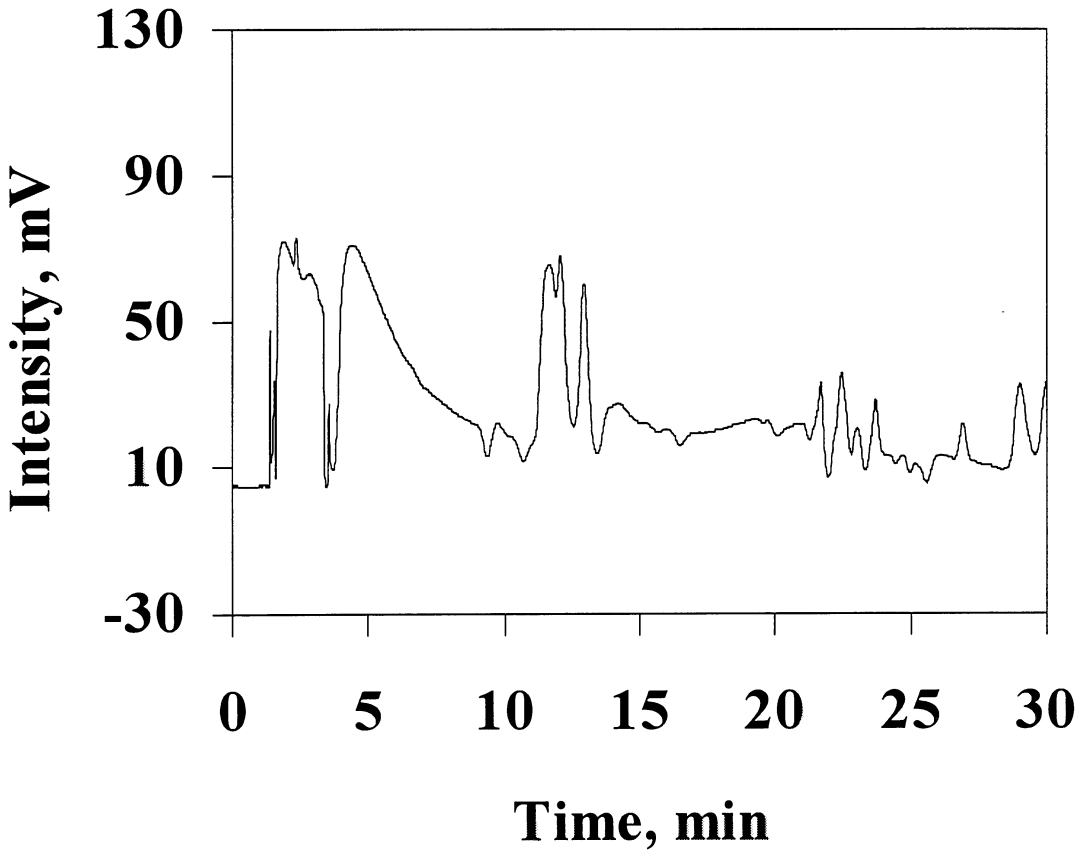

Figure 17. Chromatogram showing sulfur-bearing gases for a sample taken with tube flush with waterwall surface inside the boiler in the "corrosive area."

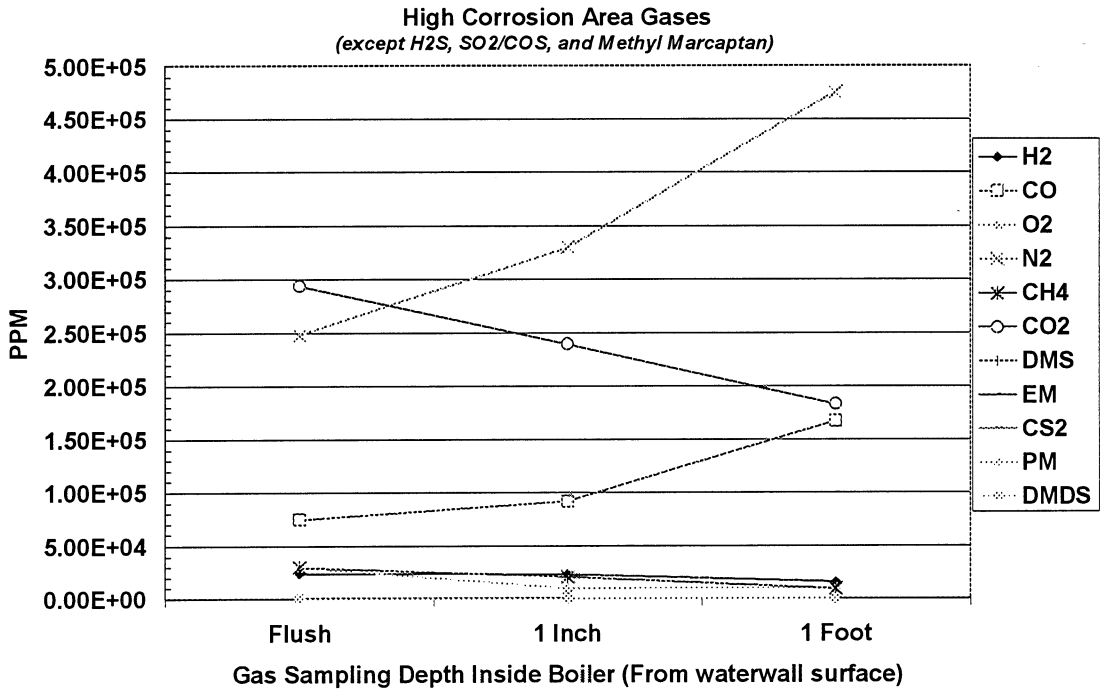

Figure 18. Concentration gas species in the samples collected from different locations inside the recovery boiler in high corrosion area.

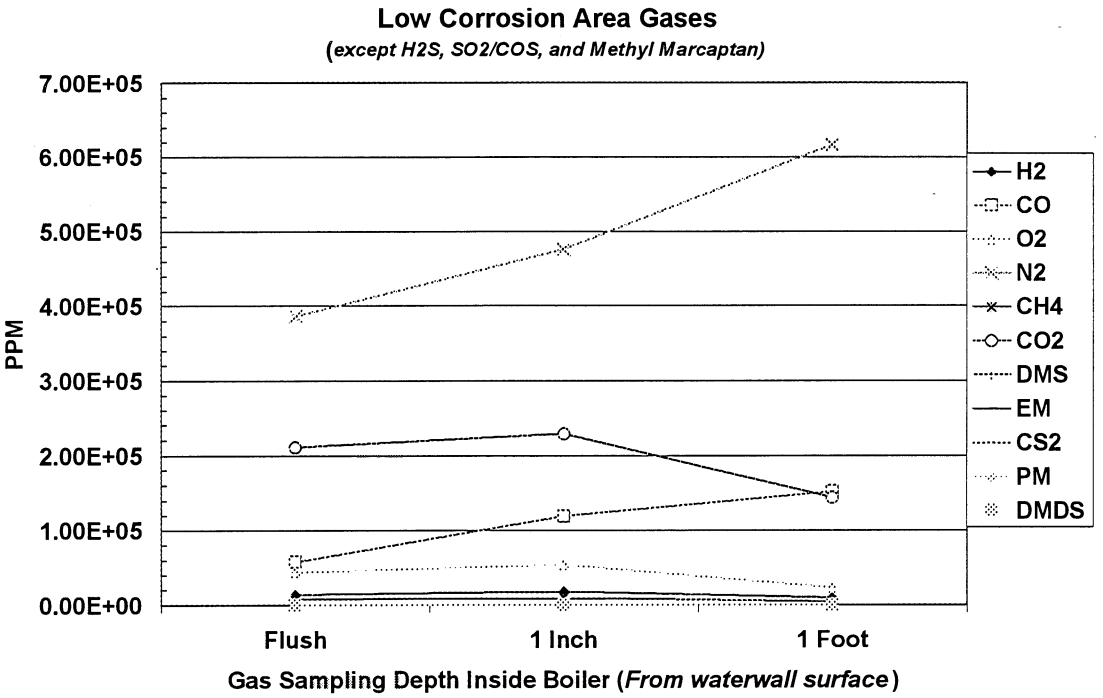

Figure 19. Concentration gas species in the samples collected from different locations inside the recovery boiler in low corrosion area.

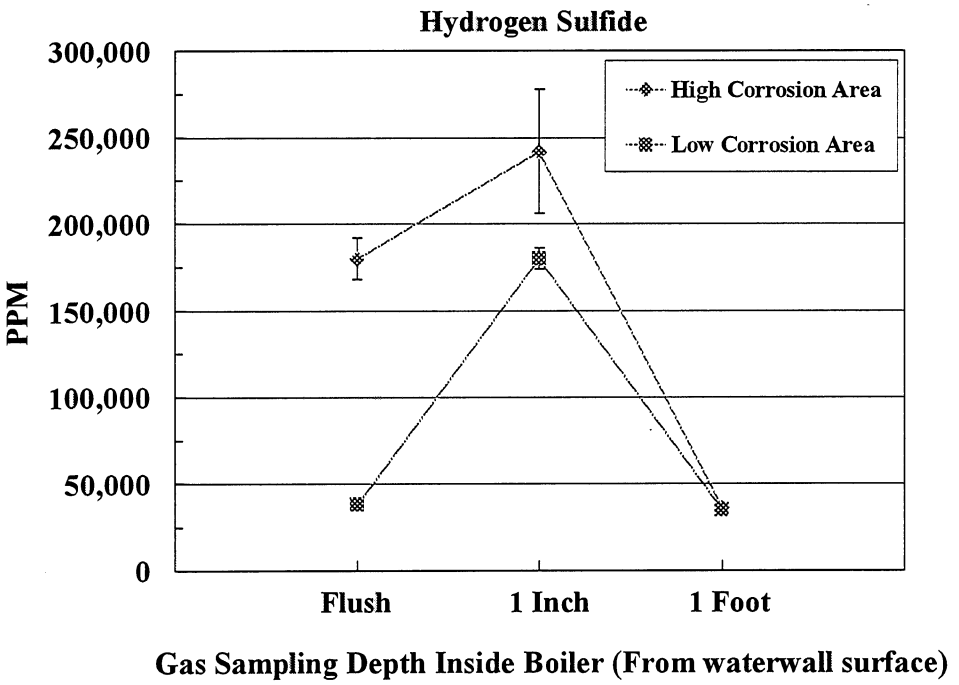

Figure 20. Concentration H_2S in the samples collected from different locations inside the recovery boiler in high corrosion and low corrosion areas.

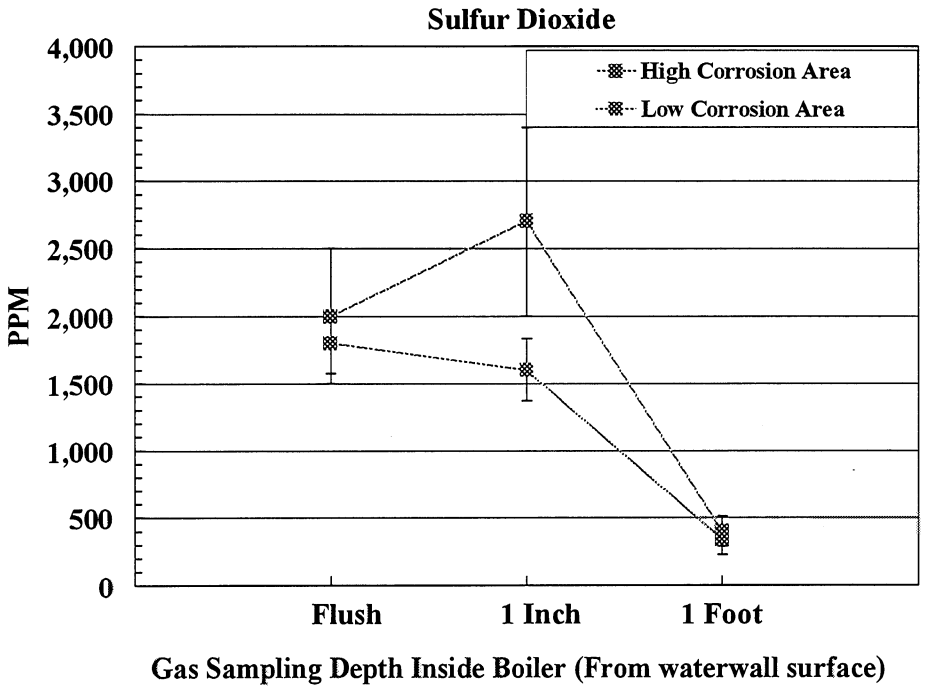

Figure 21. Concentration SO_2 in the samples collected from different locations inside the recovery boiler in high corrosion and low corrosion areas.

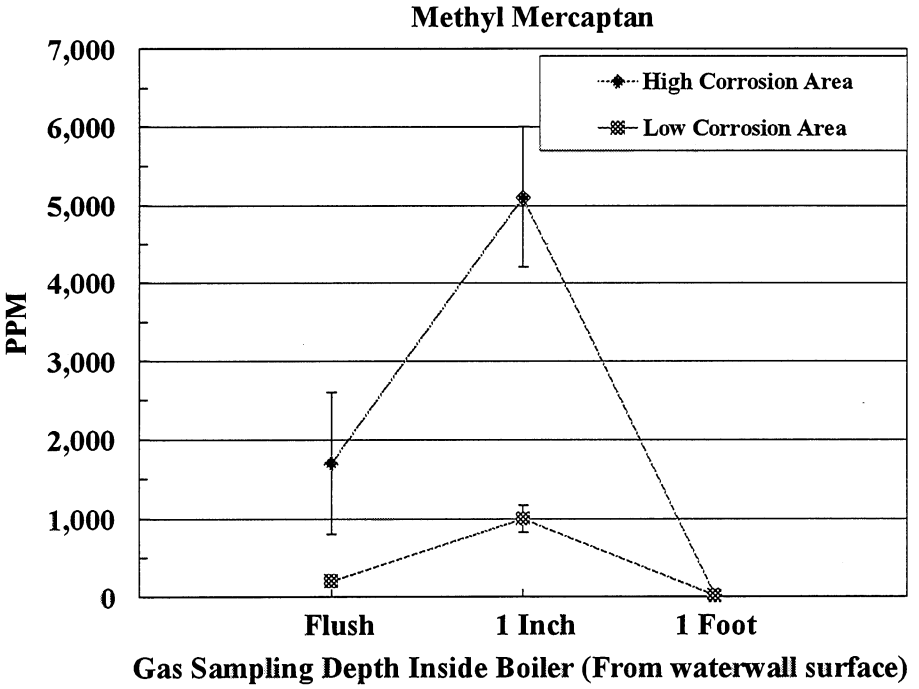

Figure 22. Concentration CH_3HS in the samples collected from different locations inside the recovery boiler in high corrosion and low corrosion areas.

Kinetics of Carbon Steel Corrosion Reaction in Different Sulfur-Bearing Gases

Thermobalance was used to study corrosion kinetics of carbon steel in different sulfur-bearing gas mixtures. Experimental procedures used in this study were similar to the ones decribed in previous PAC reports (1997 and 1998). Weight changes were monitored continuously while the test was in progress. Two gas mixtures have been tested for a fifteen day period. Individual gases to be tested in this program include the gases identified from the gas analysis done on kraft recovery boiler gases extracted from the lower furnace areas.

Weight gain with test time for the tests carried out in 1% H_2S or 1% COS are shown in Figure 23. Hydrogen sulfide produced 2.5 times higher weight gain than that of COS. Decomposition of COS to produce sulfur gas also produces carbon monoxide, which is a reducing agent, and that will affect the sulfidation of iron.

Similar tests will also be carried out for sulfur dioxide, methyl mercaptan, ethyl mercaptan, and dimethyl sulfide to establish a baseline data. After establishing baseline values, individual gases will be mixed in the ratios found in the recovery boiler, lower furnace, gases at the waterwall surface in corrosive areas, and waterwall materials like c-steel, 304L will be tested in this mixture at relevant temperatures.

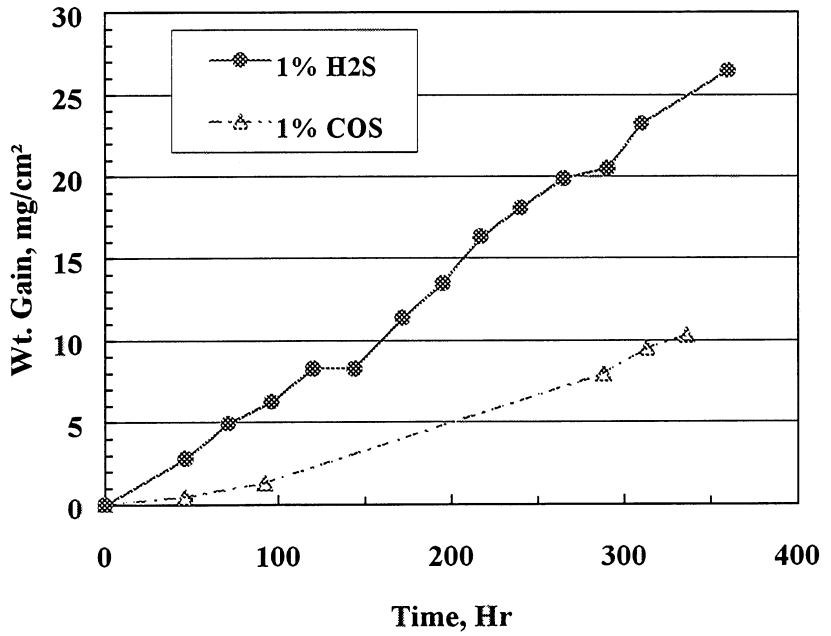

Figure 23. Continuous monitoring of weight gain of SA-210 carbon steel specimen during 15-day thermobalance tests at 320° in 1% H_2S and 1% COS.

Stress Corrosion Cracking of 304-L Stainless Steel in Kraft Recovery Boilers

Project Title: Stress Corrosion Cracking of Composite Tubes in Kraft Recovery Boilers

Project Staff: Preet Singh, Jamshad Mahmood

Project Funding: Oak Ridge National Laboratory

OBJECTIVES :

To study environments in kraft recovery boilers that may cause stress corrosion cracking of 304-L stainless steels.

INTRODUCTION :

Composite tube cracking in kraft recovery boilers is one of the major safety concerns of recovery boilers. Results of the ORNL investigation and other published results indicate that the composite tube cracking in kraft recovery boilers may be due to SCC. It is not clear which environments are responsible for these failures.

Composite tubes with outer layer of 304-L and inner shell of c-steel are used in the lower furnace and boiler floor of the kraft recovery boilers. In recent years, a number of composite tube failures have been reported. Failure analysis of these tubes, conducted at ORNL and by other researchers, indicates that SCC may be the major factor in these failures. All circumstantial evidence leads us to a hypothesis that stress corrosion cracking during shutdown of the boiler may be the prime cause of the failure of composite tubes in recovery boilers. One of the corrosive environments under scrutiny is the wash water, which is a smelt solution. Local composition and concentration of the wash water may vary from area to area in the same boiler. The project at IPST was started to understand the susceptibilities of 304-L stainless steel in wash water and its constituents.

Experimental Procedures:

Slow Strain Rate Tests

Stress corrosion cracking susceptibility of 304-L stainless steel in different wash water compositions and temperatures was studied. 304-L tensile specimens were tested using the slow strain rate test method. Gage length of the tensile specimen was exposed to the test environment and the specimens are strained at a constant extension rate giving very slow ($< 1x10^{-6}s^{-1}$) initial strain rates. Specimens were generally tested till they fractured. There

are a number of different parameters that can be compared to quantify these results (i.e., % reduction in area, % elongation, crack velocity, etc.). However, the presence of stress corrosion cracks on the specimen surface and/or fracture surfaces are of prime importance.

Figure 24 shows an example of a specimen with stress corrosion cracks on its surface, whereas, Figure 25 shows an example of a specimen with ductile fracture, without any stress corrosion cracks. After the tests were complete, the specimens were examined for surface cracks and the crack depth measurements were made. One half of the specimen was sectioned, mounted, and polished to measure crack lengths and examine the mode of cracking.

Constant Extension Tests

Constant extension or constant strain tests were done in (Na_2S + NaOH) solution to determine the threshold strain required to initiate a stress corrosion crack in this system and to establish the effects of applied total strain on the crack growth rate in this system. In these tests, the specimens were strained to a given initial strain and the strain was held constant for 24 hours. After 24 hours of exposure, the specimens were examined for surface cracks, sectioned, mounted and polished to measure crack depths.

Table IV. Composition of Artificial Wash Waters Tested in These Tests

Chemicals	Artificial WW#1	Artificial WW#2	Artificial WW#3
Sodium Carbonate	65%	60.50%	33.333%
Sodium Sulfate	17%	14%	
Sodium Sulfide	15%	15%	33.333%
Sodium Thiosulfate	2%	5%	
Sodium Chloride	0.50%	5.00%	
Sodium Hydroxide	0.50%	0.50%	33.333%

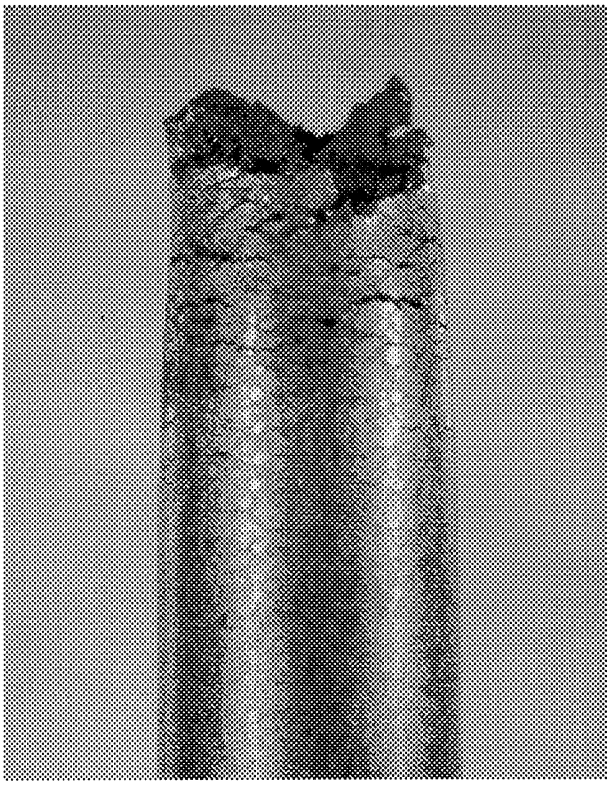

Figure 24. Micrograph of test specimen # 30 showing stress corrosion cracks on a tensile specimen tested at slow strain rate.

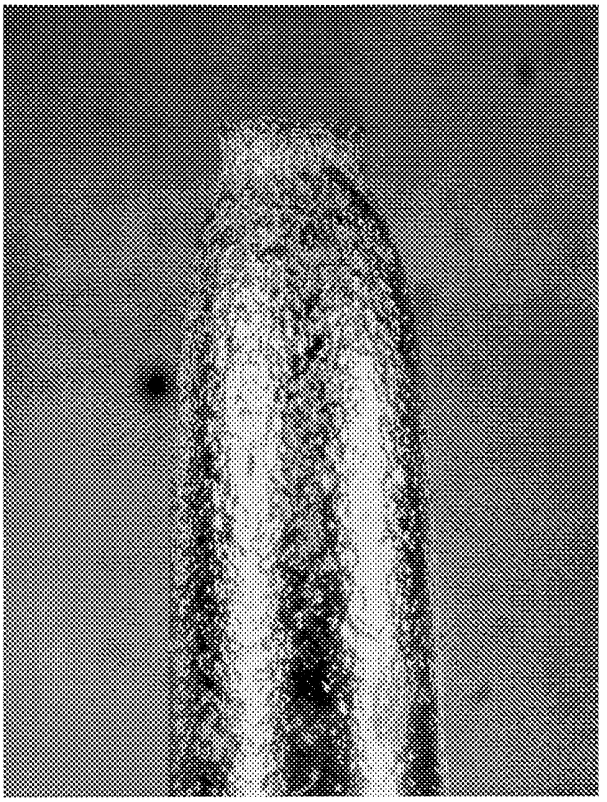

Figure 25. Micrograph of test specimen # 28 showing ductile fracture (no stress corrosion cracking) on a tensile specimen tested at slow strain rate.

Summary of Results:

Washwater # 1

A series of tests was conducted in artificial wash water #1. Tests conducted below temperatures of 200°C did not show any signs of SCC, as shown in Table V. Specimens tested at higher temperatures showed severe SCC in this environment. Cracks were transgranular branched cracks, as shown in Figure 26. Some tight unbranched transgranular cracks were also found on the specimens in areas away from the final fracture. Tests were also carried out with applied potential, as shown in Table V. 304-L specimens tested with applied potential in the test range did not show any SCC in washwater #1. Further tests are planned to cover a broad range of potential values to establish the electrochemical conditions required for SCC in this system.

Table V. Slow Strain Rate Test Data for Specimens Tested in Washwater #1

SP#	Test Solution	Temp. °C	E, mv (SCE)	Remarks
13	Artificial WW # 1	90	OCP	No Crack
14	Artificial WW # 1	200	OCP	Multiple SCC Cracks
16	Artificial WW # 1	150	OCP	No Crack
20	Artificial WW # 1	200	OCP	Multiple SCC Cracks
22	Artificial WW # 1	200/90	OCP	No Crack
24	Artificial WW # 1	200/150	OCP	Multiple SCC Cracks
Applied Potential Tests				
25	Artificial WW # 1	100 C	-0.740	No Crack
29	Artificial WW # 1	100 C	-0.650	No Crack
32	Artificial WW # 1	100 C	-0.100	No Crack
35	Artificial WW # 1	90 C	-0.850	No Crack
36	Artificial WW # 1	90 C	-0.950	No Crack
41	Artificial WW # 1	90 C	-0.740	No Crack
44	Artificial WW # 1	90 C	-0.100	No Crack
47	Artificial WW # 1	90 C	-0.650	No Crack
48	Artificial WW # 1 (P.H 13.938)	90 C	-0.900	No Crack
51	Artificial WW # 1	90 C	-0.740	No Crack

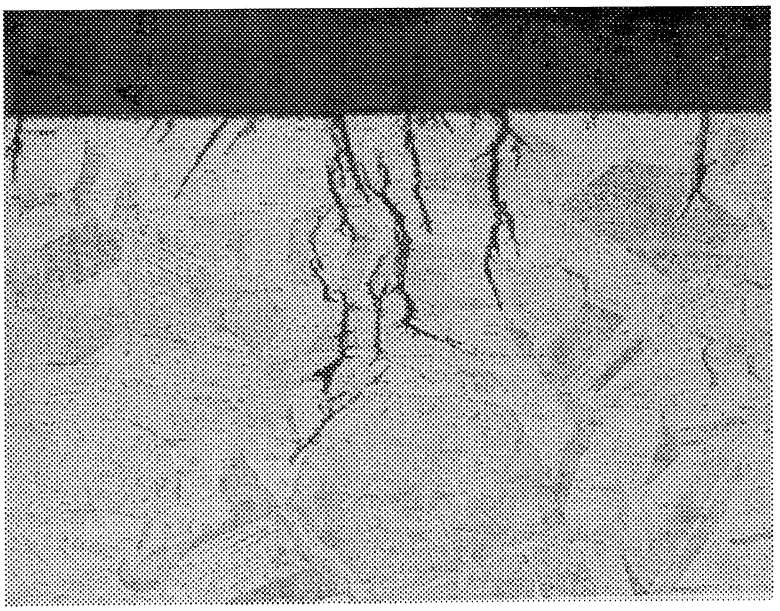

Figure 26. Optical micrograph showing transgranular branched stress corrosion cracks.

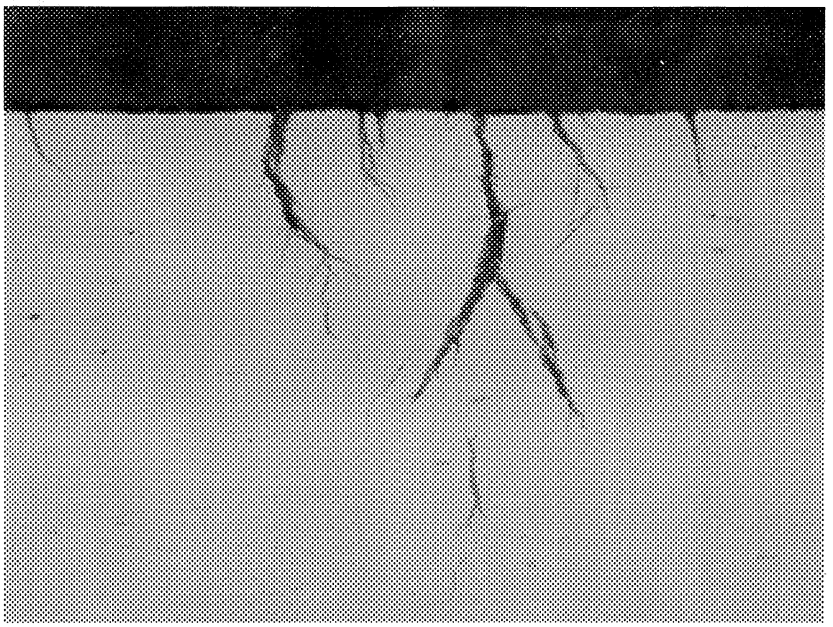

Figure 27. Optical micrograph showing branched stress corrosion cracks.

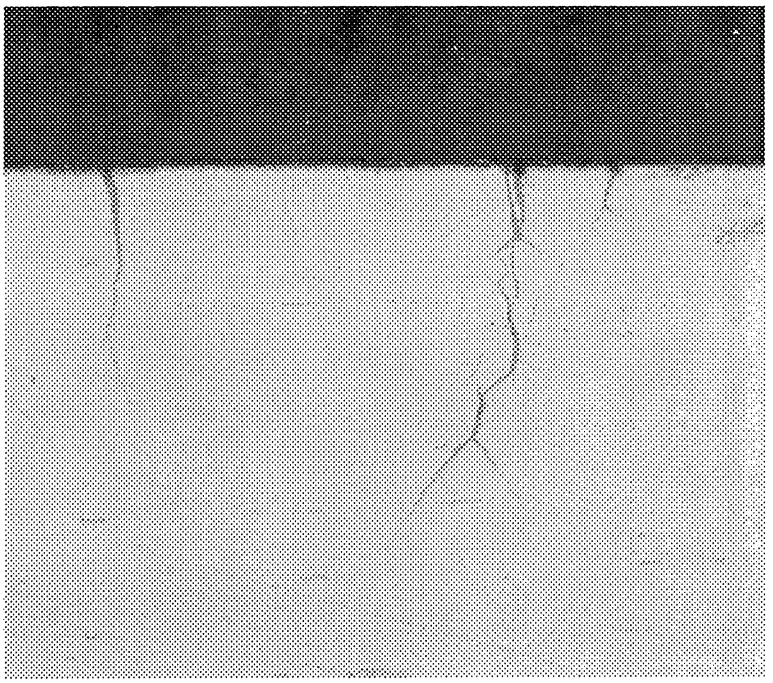

Figure 28. Optical micrograph showing branched and tight unbranched transgranular stress corrosion cracks.

Washwater #2

A series of tests were conducted in artificial wash water #2 that had higher chloride and thiosulfate concentrations than wash water #1. Again as for tests in wash water #1, tests conducted below temperatures of 200°C did not show any signs of SCC, as shown in Table VI. Specimens tested at 200°C showed severe transgranular SCC in this environment.

Table VI. Slow Strain Rate Test Data for Specimens Tested in Wash Water #2

SP#	Test Solution	Temp. °C	E, mv (SCE)	Remarks
15	Artificial WW # 2	90	OCP	No Crack
33	Artificial WW # 2	150 C	OCP	No Crack
34	Artificial WW # 2	200 C	OCP	Multiple SCC Cracks
Applied Potential Tests				
39	Artificial WW # 2	90 C	-0.950	No Crack
40	Artificial WW # 2	90 C	-0.850	No Crack
42	Artificial WW # 2	90 C	-0.650	No Crack
43	Artificial WW # 2	90 C	-0.100	No Crack

Wash water #3

Wash water #3 had higher amounts of sodium hydroxide and sodium sulfide compared to #1 and #2 wash waters. A series of tests was conducted in artificial wash water #3 and the results are listed in Table VII. In the presence of higher NaOH and higher Na_2S, even the specimen tested at 150°C showed tight branched transgranular SCC under open circuit conditions. Tests done at 125°C or below did not show any signs of SCC.

Table VII. Slow Strain Rate Test Data for Specimens Tested in Wash Water #3

SP#	Test Solution	Temp. °C	E, mv (SCE)	Remarks
26	Artificial WW # 3	200C	OCP	Multiple SCC Cracks
30	Artificial WW # 3	200C	OCP	Multiple SCC Cracks
46	Artificial WW # 3	150 C	OCP	Multiple SCC Tight Cracks
49	Artificial WW # 3	125 C	OCP	No Crack
50	Artificial WW # 3	100 C	OCP	No Crack
Applied Potential Tests				
27	Artificial WW # 3	100 C	-0.740	No Crack
28	Artificial WW # 3	100 C	-0.650	No Crack
37	Artificial WW # 3	90 C	-0.850	No Crack
38	Artificial WW # 3	90 C	-0.950	No Crack
45	Artificial WW # 3	90 C	-0.100	No Crack
53	Artificial WW # 3	90 C	-0.650	No Crack
54	Artificial WW # 3	90 C	-0.740	No Crack

Individual Constituents of Washwater and their Combinations

Individual constituents of wash water as well as simple mixtures of different constituents of wash water were tested to study their influence on the SCC of 304L at temperatures of 100°C or below. As shown in Table VIII, Na_2S solutions tested at 25, 90 or 100°C did not show any signs of corrosion or SCC, as is expected. However, concentrated (~30%) NaOH solution at 100°C did show tight transgranular SCC. When Na_2S was present with NaOH in the solution, the cracking could be found at temperatures as low as 50°C.

Specimens, that had stress corrosion cracks after slow strain rate tests also had a black film on the surface. On most of these specimens the film was shiny-black film, however, some specimens had a dull-black film as well. The film was very similar in appearance to the magnetite film formed on the surface of carbon steels. We are conducting some tests to identify this film so that we can understand the environmental and electrochemical conditions that may cause SCC of 304-L stainless steels in kraft recovery boilers during shutdown conditions.

Table VIII. Slow Strain Rate Test Data for Specimens Tested in Test Solutions Described in Table

SP#	Test Solution	Temp. °C	E, mv (SCE)	Remarks
4	(1N)Na_2S 9H_2O	25	OCP	No Crack
7	(1N)Na_2S 9H_2O	25	OCP	No Crack
8	(1N)Na_2S 9H_2O	102	OCP	No Crack
3	(1N)Na_2S 9H_2O	90	OCP	No Crack
17	Crystals of Na2S and H2O (Saturated sol.)	100	OCP	No Crack
58	90gm Na_2S + 300 ml H2O	100 C	OCP	No Crack
6	(1N)Na_2S 9H_2O +Na_2CO_3	25	OCP	No Crack
5	(1N)Na_2S 9H_2O +Na_2CO_3	90	OCP	No Crack
21	300 gms NaOH + 50 ml H_2O	100	OCP	No Crack
57	90gm NaOH + 300 ml H_2O	100 C	OCP	Multiple SCC Tight Cracks
61	90gm NaOH + 300 ml H_2O	75 C	OCP	No Crack
19	150 gm Na_2S+150 gm NaOH +50 ml H_2O	100	OCP	Multiple SCC Cracks
23	150 gm Na_2S+150 gm NaOH +50 ml H_2O	100 C	OCP	No Crack
31	150 gm Na_2S+150 gm NaOH +50 ml H_2O	75 C	OCP	No Crack
52	150 gm Na_2S+150 gm NaOH (No H_2O)	100 C	OCP	No Crack
55	150 gm Na_2S+150 gm NaOH +75 ml H_2O	100 C	OCP	Multiple SCC Cracks
56	150 gm Na_2S+150 gm NaOH +75 ml H_2O	100 C	OCP	Multiple SCC Cracks
59	150 gm Na_2S+150 gm NaOH +75 ml H_2O	75 C	OCP	Multiple SCC Cracks
60	150 gm Na_2S+150 gm NaOH +75 ml H_2O	75 C	OCP	Multiple SCC Cracks

Constant Extension Tests

Figure 29 shows results from the constant strain tests where the graph indicates % strain on the X-axis, which was calculated from the displacement data and not by using an extensiometer. However, data clearly indicate that the threshold strain for the initiation of SCC in this system is around yield point of the material.

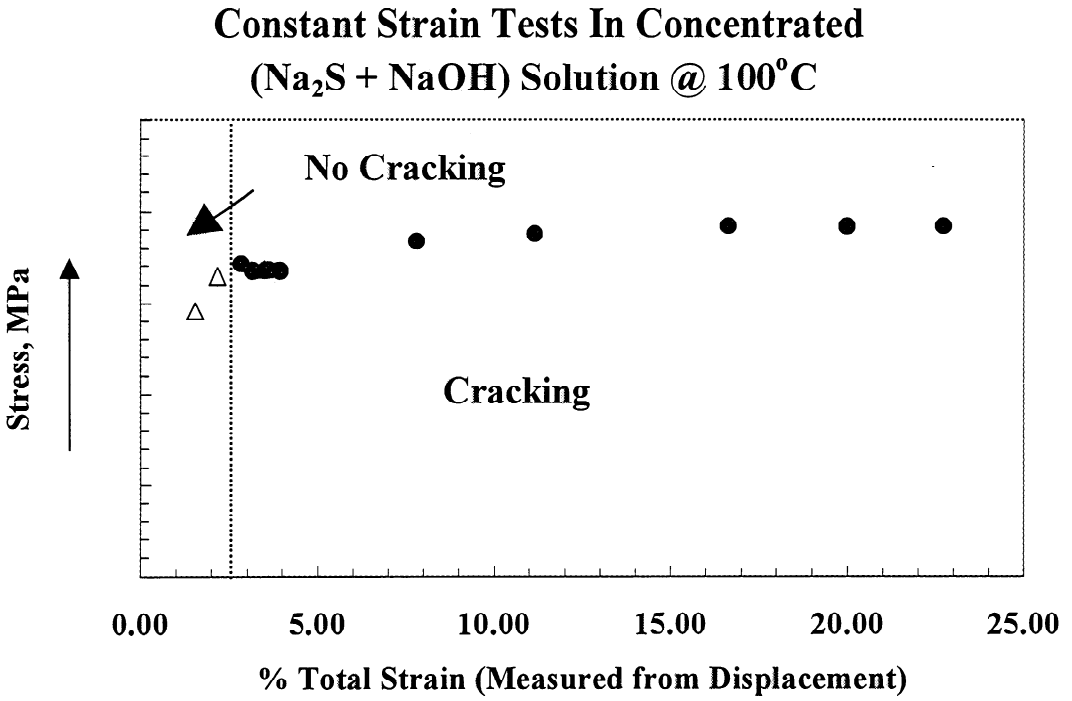

Figure 29. Results from constant extension tests. Open symbols indicate no-cracking at that strain, whereas closed symbols indicate SCC.

Conclusions

1. Results from wash water #1 and #2 show that 304-L stainless steel does not undergo stress corrosion cracking at temperatures up to 150°C. However, at 200°C severe stress corrosion cracking was noticed under tested open circuit conditions.

2. Applied potential tests did not produce conditions required for stress corrosion cracking. Further tests under controlled potential will be conducted to understand the mechanism of this phenomenon.

3. Results, so far, indicate that the presence of higher concentrations of hydroxides can lead to transgranular stress corrosion cracking.

4. In the presence of sulfides, hydroxides can cause cracking at lower temperatures (50°C) than required for pure hydroxide solutions (100°C or more).

5. Black surface film is associated with the stress corrosion cracking of 304-L specimens under all of the tested conditions. Work is continuing to characterize this film to understand the mechanism of cracking in the kraft recovery boilers.

6. The threshold stress/strain for the initiation of SCC is around yield point of the material.

CORROSION IN CLOSED CYCLE MILLS

PROJECT F019

ANNUAL RESEARCH REVIEW

March 24, 1999

Preet M. Singh
Gregory J. Fonder
Jamshad Mahmood
Sloane Stalder

Institute of Paper Science and Technology
500 10th Street, N.W.
Atlanta, GA 30318

TECHNICAL PROGRAM REVIEW

Project Title:	CORROSION IN CLOSED CYCLE MILLS
Project Number:	F019
Division:	Chemical and Biological Sciences
Project Staff:	P. Singh, G. Fonder, Jamshad Mahmood, S. Stalder
FY 97-98 Budget:	$119,079

PROGRAM OBJECTIVES

To identify key corrosion and materials-related issues, which may impact the successful implementation of various closed mill scenarios and provide support to maximize the potential of these new technologies.

INTRODUCTION

The main objective of this project was to study the effects of mill closure on corrosion of equipment in contact with white water. Effects on any particular equipment will depend upon the material used as well as on the environment which comes in contact with this material. The following environmental changes are expected in a closed system:

1. Increase in temperature due to re-circulation of warm water. Temperature increase will depend upon the degree of closure and other process parameters. However, this increase is not expected to be more than 10-20°C in most areas of the white water system.

2. Changes in the chemical composition are expected. These changes will depend upon the papermaking process, and strategies applied to mill closure. Concentrations of chemicals, which enter the white water system with pulp but do not leave with the paper product, are expected to increase in closed white waters, unless they are actively removed from the system. Some of these chemicals may even reach solubility limits and then precipitate out as scale or loose insoluble products in the white water. Whereas, concentration of other chemicals, that era intentionally added during the papermaking process can be controlled to some extent. This may not be possible in cases where a certain concentration of chemicals have to be added at a particular stage of the papermaking process. However, concentrations of chemical species in the closed white water are expected to be higher than in the open white waters.

3. White water closure may also lead to changes in pH, which in-turn will depend upon the initial pH and chemical changes.
4. Accumulation of dissolved organic species like starch may lead to increased microbial activity. This, in turn, can lead to microbial corrosion in the white water system.

All of the above stated environmental changes can affect the corrosivity of white water. Corrosivity of closed white water will depend upon various process parameters and design of mill closure.

There is a considerable amount of published literature on microbial corrosion in the paper mills. These papers include description of the problem as well as some of the remedial methods that can be applied to mitigate this problem or avoid it before it occurs. A bibliography of these papers is included in this report at the end of this section. Temperature changes in closed white water systems may affect microbial growth. This will depend upon the final temperature and metabolic nature of microbes in question. Increased microbial activity may lead to an increase in microbiological corrosion.

It is not practical for this project to verify the material behavior in every possible closed white water scenario, so an experimental program was designed to answer the following concerns:

- How will different materials perform in concentrated white water solutions, assuming that the concentration of major inorganic constituents of white water will increase in a closed mill closure? This situation can also arise in the open white waters in the areas where concentrations can buildup due to alternate immersion or evaporation of water.

- How will different materials behave in fog/mist areas of paper machines in closed white water systems?

- What will be the effect of increased chemical composition on fatigue behavior of roll materials, especially the effects on threshold stress intensities and crack growth rates?

Experimental Procedures

Experiments for this project were designed to study the effects of white water closure on the materials. Tested materials include alloys commonly used in the paper machine areas (i.e., 304-L, 316-L, and 317-L) and other alloys that are less commonly used but are known to be more resistant to corrosion in similar environments (i.e., 654 SMO, 254 SMO, SAF 2205, SAF 2507). Two types of laboratory tests are planned for this project; submerged coupon exposure tests, and salt spray exposure of coupons in fog chamber in different white water solutions.

Table X shows the test matrix of different white water compositions being used for various tests. The white water compositions were chosen with an objective of determining the concentration limits that can be safely handled by a given material.

Table X. Simulated White Water Solutions Compositions

Environment	pH	Cl^- ppm	SO_4^{-2} ppm	$S_2O_3^{-2}$ ppm
Base Line – pH4	4.0	200	500	50
Strong Solution-10 – pH4	4.0	2000	5000	500
Base Line – pH9	9.0	200	500	50
Strong Solution-10 – pH9	9.0	2000	5000	500

Immersion Tests with Crevice Coupons

Seven different materials: 654 SMO, 254 SMO, SAF 2205, SAF 2507, 304L, 316L, 317L were used in this study. One side of each coupon was polished to 1000-grit finish whereas the other side of the coupon had 120-grit finish. Individual racks were assembled with one coupon of each material in each rack, as shown in Figure 30. Every coupon had a serrated crevice washer on each surface. Precautions were taken to eliminate any galvanic contact between the bolt holding the crevice washers and the coupon or within different coupons. To study the effects of cold work on corrosion susceptibility of the tested materials, three small cold-worked areas were also stamped on each side of the coupon. Coupons will be tested for 15 days, one month, three months, six months, and one year.

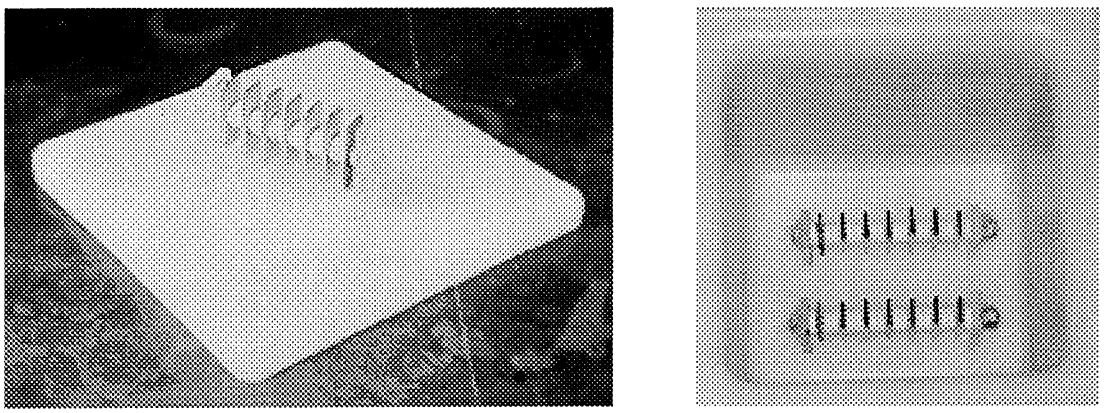

Figure 30. Pictures of a) coupon racks and b) containers used to expose them in a given environment used in this study.

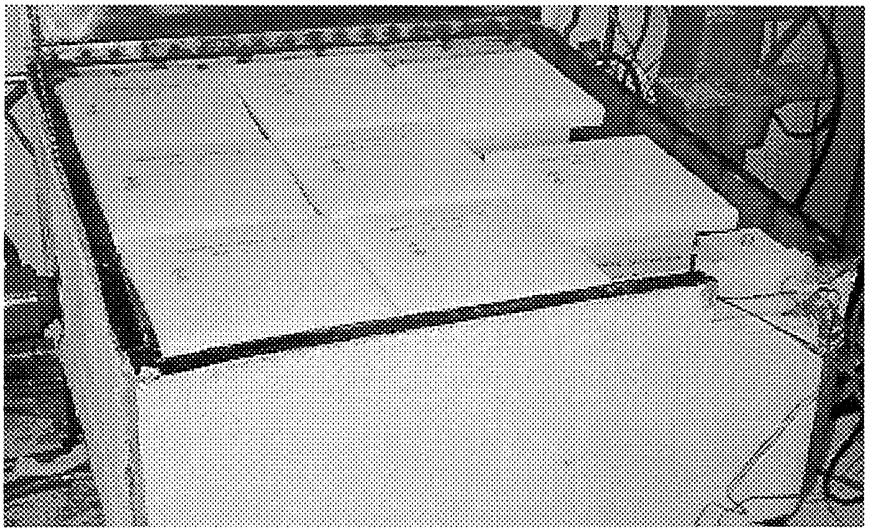

Figure 31. Constant temperature water bath with containers used to expose crevice coupon racks.

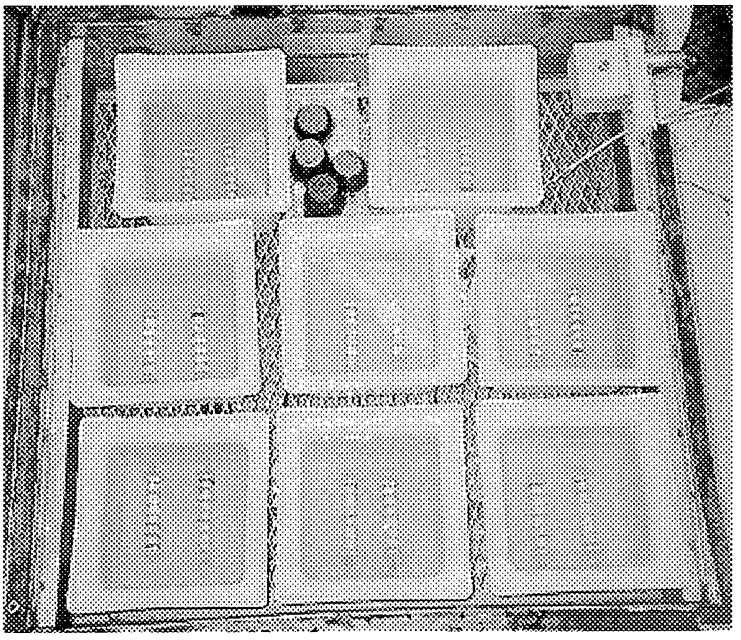

Figure 32. Containers with test solution and coupon racks in the temperature water bath.

Sixteen individual racks were prepared for a given temperature. Volume of the solution in each test container was more than 25 ml/inch^2 of the exposed coupons, as recommended by the ASTM G48-97 standard practice. Test solutions were refreshed every day for the first week. Thereafter, solutions were changed every three days for the next two weeks, and after one week after the third week. Waterbath and the containers with test solutions are shown in Figures 31 and 32, respectively.

Chemical analysis was performed after different time periods to quantify the changes in the composition of white water changed with time. Chemical analysis was performed on the fresh white water solution, solution used for coupon exposure, and the solution kept in the water bath but not exposed to test coupons. Results from these analysis are listed in Appendix I. Chemical analysis has shown that that there was no measurable change in the composition of white waters at exposure temperatures over a two-week period. However, ICP analysis has indicated that there were corrosion products in the exposed solutions. In high pH (9.0) simulated white waters, precipitated corrosion products were seen at the bottom of the container. Solution was collected from the top and bottom of this container and analysis clearly indicated that the bulk of the solution did not have significant soluble metals, whereas the bottom samples for pH-9 solutions showed high concentrations of metal. Concentrations were found to be higher in the concentrated solutions than in the baseline TAPPI-D waters. These precipitates were insoluble hydroxides of iron, nickel and chromium and were only found under 304L specimens and started to appear after about two days of exposure. Other specimens did not show any visible signs of corrosion on their surface in the first two weeks of exposure. Long term tests are still under way.

Salt Spray tests in Fog chamber

Certain areas of the paper machine are exposed to continuous fine spray/mist of white water. With mill closure, composition of this environment is also expected to change. Corrosion susceptibility of metals in spray/mist of an environment can be significantly different from submerged metals in a similar environment. This study was started to characterize the corrosion behavior of various materials exposed to simulated white water under fine spray conditions in the fog chamber.

The salt spray cabinet is a deep, temperature-controlled chest, as shown in Figure 33, equipped with a spray-tower that makes a fine mist of the salt solution. The spray droplets are directed upward so that they fall onto metal specimens below, rather than being sprayed directly onto them. Graduated cylinders are placed in corners of the cabinet to make sure that all specimens receive the same amount of mist. Simulated white water that falls at the bottom of the cabinet is discarded; all spray/mist coming from the spray-tower is from the fresh white water solution.

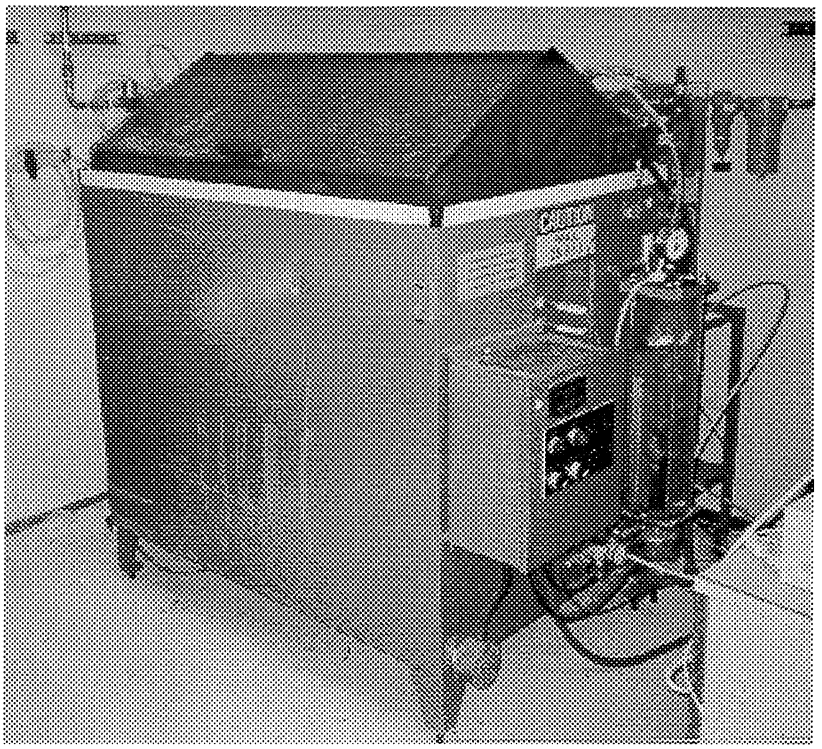

Figure 33. Fog Chamber used to perform salt spray tests

Test coupons used for salt spray cabinet testing were made from eight different materials: 654 SMO, 254 SMO, SAF 2205, SAF 2507, 304L, 316L, 317L and carbon steel. A typical coupon used in this study is shown in Figure 34. All coupons of a given material were cut from the same metal sheet to avoid any heat to heat variation in the tested coupons. Cold-worked edges, developed by sheet cutting operation, were removed from the coupons by milling 1/8 inch of material was cut from the edges of the coupon. Each coupon for these tests also had serrated crevice washers on either side of the coupon. Precautions were taken to eliminate any galvanic contact between bolt holding crevice washers and the coupon. Each coupon was polished on one side to 1700-grit finish, whereas the other side of the coupon was left with as-received mill finish. To study the effects of cold work on corrosion susceptibility of the tested materials, five small cold-worked areas were also stamped on the finished side of the coupon.

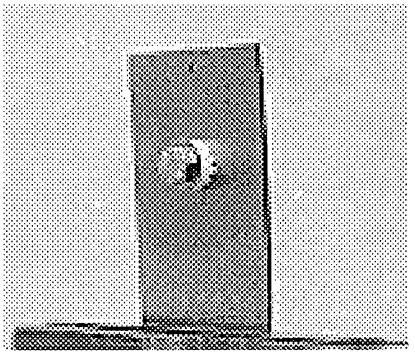

Figure 34. Coupons with crevice washers, and cold-worked spots, used in Fog Chamber test.

Salt spray tests were performed in accordance with the ASTM B-117 procedure for Salt Spray Testing. It has been modified so that simulated white waters are used instead of the salt solution suggested by the ASTM procedure. During testing, each coupon was placed in the salt spray cabinet by suspending it by coated wire from a plastic rack. It was ensured that the coupons were below the level of the spray tower to prevent direct misting onto the coupons. Care was also taken to avoid a coupon touching its neighbor, and to prevent condensate from one coupon falling onto another.

Test durations of 15, 30, 90 and 180 days are planned, using triplicate coupons of each material for each test condition. Compositions of the white waters used in this study are given in Table XI.

Table XI. Simulated White Water Solutions Compositions

Environment	Cl^- ppm	SO_4^{-2} ppm	$S_2O_3^{-2}$ ppm
Base Line (TAPPI -D)	200	500	50
Strong Solution-10	2000	5000	500

RESULTS AND DISCUSSION:

Fifteen-Day Exposure Tests

One set of coupon racks was removed from each of the four tested white waters after fifteen days. Long-term tests are in progress and the results from those tests will be incorporated in our next PAC report. Test coupons were designed to answer the following concerns:

1. General corrosion susceptibility (Not a big concern for stainless steel coupons)
2. Crevice corrosion susceptibility
   - Initiation time
   - Probability of crevice attack.
3. Pitting tendency on the exposed surface
4. Effect of environment on the exposed edges of rolled material, especially the role of inclusion morphology on pitting of edges
5. Effect of cold work on initiation of localized corrosion
6. Effect of surface finish on all of above stated corrosion phenomena

Figure 35 shows coupons exposed to four different environments (i.e., two acidic white waters and two alkaline white waters). Figure 35 shows 120-grit polished surface. This picture was taken before cleaning the specimens for further detailed examination and quantification. It is clear from this picture that the 304-L specimens were covered with dark corrosion film, dark brown in color. 304-L specimens showed crevice corrosion on the rough surface in all tested environments, as is shown by the data in Table XII. 316-L specimens exposed to strong solution-10 with pH-4 also showed crevice initiation. However, none of the other exposed specimens showed any signs of crevice corrosion in fifteen days.

304-L specimens also showed pitting on the general surface in all of the tested environments. However, the pitting tendency was more severe on the rough surfaces compared to the smooth surface, polished to 1200-grit. These results are listed in Table XIII. The edges of these specimens had more pitting on their smaller edges that were perpendicular to the rolling direction of the specimens. This observation is in accordance with the expected behavior, as intersection of sufide inclusions on the surface in this direction will lead to selective pit initiation. This confirms that if a rolled 304-L stainless steel plate is exposed to these environments then the exposed edges are more prone to pitting attack than the general surface.

General corrosion was not detected on any of the coupons. Although there was weight change in the exposed coupons, it has not been quantified as it is inappropriate to quantify general corrosion from such data in a case where localized attack is prominent.
Cold worked spots did not show any unusually high tendency for corrosion compared to the general surface. However, pitting attack was found at the edges of these cold worked spots. Tests for the longer time periods are going on. We will hold our discussion and conclusion till we collect the rest of the data from these tests.

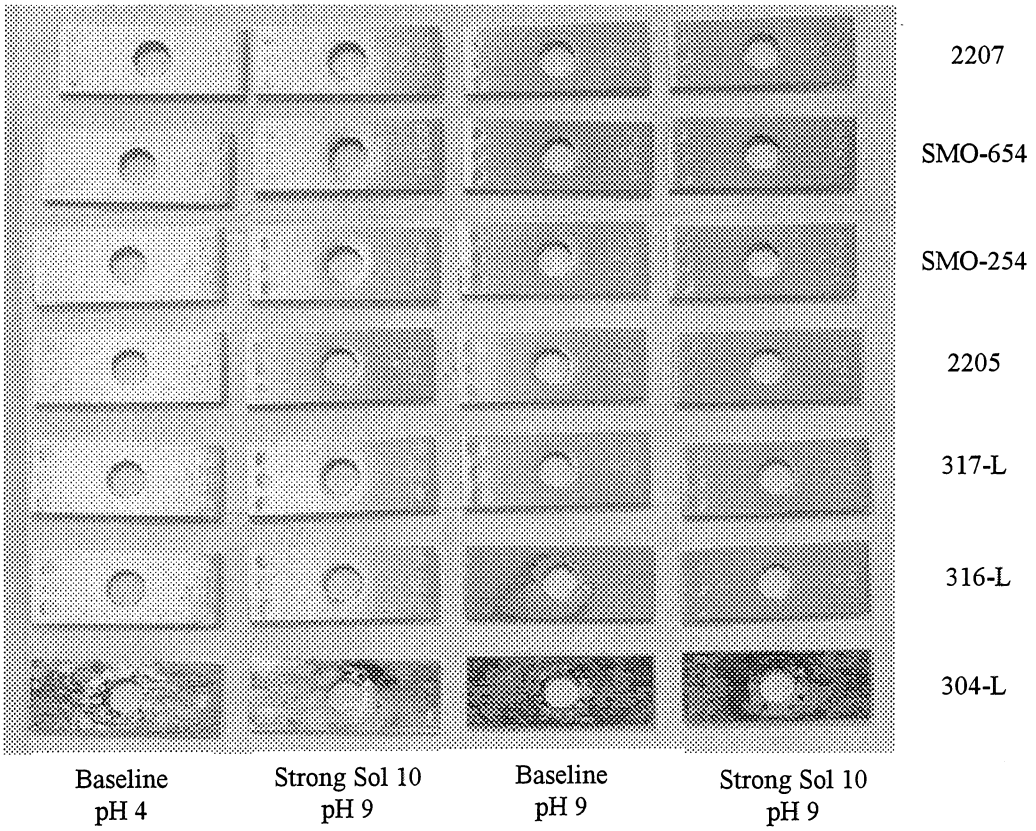

Figure 35. Coupons after fifteen days of exposure at 160°F, to different white waters, as indicated by the labels in the picture. Surface with 120-grit is shown in this picture.

Table XII. Results from crevice coupons exposed to different white water environments for fifteen days.

Material	Test Solution	pH	Temp °F	Crevice Attack on Rough Surface	Crevice Attack on Smooth Surface
304-L	Baseline pH 4	4.0	160	10/12	0/12
316-L	Baseline pH 4	4.0	160	0/12	0/12
317-L	Baseline pH 4	4.0	160	0/12	0/12
2205	Baseline pH 4	4.0	160	0/12	0/12
254-SMO	Baseline pH 4	4.0	160	0/12	0/12
654-SMO	Baseline pH 4	4.0	160	0/12	0/12
2207	Baseline pH 4	4.0	160	0/12	0/12
304-L	Strong Sol.-10 pH 4	4.0	160	7/12	9/12
316-L	Strong Sol.-10 pH 4	4.0	160	3/12	3/12
317-L	Strong Sol.-10 pH 4	4.0	160	0/12	0/12
2205	Strong Sol.-10 pH 4	4.0	160	0/12	0/12
254-SMO	Strong Sol.-10 pH 4	4.0	160	0/12	0/12
654-SMO	Strong Sol.-10 pH 4	4.0	160	0/12	0/12
2207	Strong Sol.-10 pH 4	4.0	160	0/12	0/12
304-L	Baseline pH 9	9.0	160	2/12	4/12
316-L	Baseline pH 9	9.0	160	0/12	0/12
317-L	Baseline pH 9	9.0	160	0/12	0/12
2205	Baseline pH 9	9.0	160	1/12	0/12
254-SMO	Baseline pH 9	9.0	160	0/12	0/12
654-SMO	Baseline pH 9	9.0	160	0/12	0/12
2207	Baseline pH 9	9.0	160	0/12	0/12
304-L	Strong Sol.-10 pH 9	9.0	160	11/12	2/12
316-L	Strong Sol.-10 pH 9	9.0	160	0/12	0/12
317-L	Strong Sol.-10 pH 9	9.0	160	0/12	0/12
2205	Strong Sol.-10 pH 9	9.0	160	0/12	0/12
254-SMO	Strong Sol.-10 pH 9	9.0	160	0/12	0/12
654-SMO	Strong Sol.-10 pH 9	9.0	160	0/12	0/12
2207	Strong Sol.-10 pH 9	9.0	160	0/12	0/12

Serrated crevice washer had 12 sections. 0/12 means that none of the sections had crevice corrosion attack, whereas 6/12 means that six sections had corrosion while the other six sections were not attacked.

Table XIII. Results showing pitting corrosion susceptibility of coupons exposed to different white water environments for fifteen days.

Material	Test Solution	pH	Temp °F	Pits on Rough Surface	Pits on Smooth Surface	Pitting on Edges
304-L	Baseline pH 4	4.0	160	HP	FP	HP
316-L	Baseline pH 4	4.0	160	NP	NP	NP
317-L	Baseline pH 4	4.0	160	NP	NP	NP
2205	Baseline pH 4	4.0	160	NP	NP	NP
254-SMO	Baseline pH 4	4.0	160	NP	NP	NP
654-SMO	Baseline pH 4	4.0	160	NP	NP	NP
2207	Baseline pH 4	4.0	160	NP	NP	NP
304-L	Strong Sol.-10 pH 4	4.0	160	HP	FP	HP
316-L	Strong Sol.-10 pH 4	4.0	160	FP	NP	FP
317-L	Strong Sol.-10 pH 4	4.0	160	NP	NP	NP
2205	Strong Sol.-10 pH 4	4.0	160	FP	NP	NP
254-SMO	Strong Sol.-10 pH 4	4.0	160	NP	NP	NP
654-SMO	Strong Sol.-10 pH 4	4.0	160	NP	NP	NP
2207	Strong Sol.-10 pH 4	4.0	160	NP	NP	NP
304-L	Baseline pH 9	9.0	160	P	NP	FP
316-L	Baseline pH 9	9.0	160	NP	NP	NP
317-L	Baseline pH 9	9.0	160	NP	NP	NP
2205	Baseline pH 9	9.0	160	NP	NP	NP
254-SMO	Baseline pH 9	9.0	160	NP	NP	NP
654-SMO	Baseline pH 9	9.0	160	NP	NP	NP
2207	Baseline pH 9	9.0	160	NP	NP	NP
304-L	Strong Sol.-10 pH 9	9.0	160	HP	FP	HP
316-L	Strong Sol.-10 pH 9	9.0	160	NP	NP	NP
317-L	Strong Sol.-10 pH 9	9.0	160	NP	NP	NP
2205	Strong Sol.-10 pH 9	9.0	160	NP	NP	NP
254-SMO	Strong Sol.-10 pH 9	9.0	160	NP	NP	NP
654-SMO	Strong Sol.-10 pH 9	9.0	160	NP	NP	NP
2207	Strong Sol.-10 pH 9	9.0	160	NP	NP	NP

FP = Few Pits (less than 10 pits on surface); Pitting = Pitting Attack (more than 10 & less than 30 pits on surface); HP = Heavy Pitting (More than 30 pits on surface); NP = No Pitting-attack

References on Microbial Corrosion in the Pulp and Paper Industry and its Prevention

1. 1997 Engineering and Papermakers: Forming Bonda for Better; *Papermaking Conference1997* Nashville, TN US(TAPPI Press): 1107-1114 (October 6, 1997; TAPPI Press).
2. Bennett, C; Control of Microbial Problems and Corrosion in Closed Systems; *Paper Technol. Ind.* 26, no. 7: 331-335 (Nov. 1985).
3. Bennett, D., Sharp, W.B.A.; Corrosion in Paper-Machine Wet Ends; *1997 Engineering & Papermakers: Forming Bonds for Better Papermaking Conference* Nashville,TN US(TAPPI Press): 481-484 (October 6, 1997; TAPPI Press).
4. Bohren, G.; SIMPSON REDUCES MACHINE DOWNTIME WITH AUTOMATED WATER DISINFECTION; Simpson Paper; Weisenfelder, J.; BetzDearborn; *Pulp & Paper* 71, no. 8: 75-76 (August 1997).
5. Bowers, D. F; CORROSION IN PAPER MACHINE SYSTEMS; *TAPPI Envir. Conf.* (Mobile) Proc.: 315-325 (April 22-24,; 1985).
6. Brozel, V. S.; Role of Sulfate-Reducing Bacteria in Microbial-Induced Corrosion; *Paper Southern Africa 9*, no. 6: 30, 32, 34, 36 (Nov./Dec.1989).
7. Cloete, T. E.; Gray, F; MICROBIOLOGICAL CONTROL IN PAPER MILLS; Paper Southern Africa 5, no. 4: 26, 28, 32 (July/Aug. 1985).
8. Corrosion Control Seminar; PIRA; UMIST., *PIRA (Leatherhead, Surrey KT22 7RU, U.K.)* SPB/5: 7 sep. paginated loose-leaf lectures (May 18, 1983).
9. Deschamps, C., Lebeault, J.M., Lenon, G.; IMPROVEMENT OF MICROBIOLOGICAL CONTROL IN CLOSED WATER SYSTEMS FOR THE PAPER AND BOARD INDUSTRY; Cent Technique du Papier; Louvel, L.; Morros, J.; Proceedings of the 1998 TAPPI International Environmental Conference & Exhibition. Part 3 (of 3): 1019-1034
10. Dexter Roger; IMPACT OF WATER CONSERVATION PRACTICES IN PAPERMAKING PROCESSES; *BetzDearborn Paper Process Group, Inc.*
11. Dhawale, S. W.; Thiosulfate: Interesting Sulfur Oxoanion That Is Useful in Both Medicine and Industry - But Is Implicated in Corrosion, Indiana University East.. *J. Chem. Educ.* 70, no. 1: 12-14 (Jan. 1993).
12. Dykstra, G. M.; GUIDELINES FOR DEPOSIT CONTROL; Buckman Laboratories International Inc.; *Sizing Short Course* (Nashville) Notes: 109-116 (TAPPI; April 8-10, 1992).
13. Flemming, H; Klahre, J.; Oekophil; Lustenberger, M.; Achilles Heel of Paper Production: Microbial Problems; *Wet-End Chemistry Conference & COST Workshop Gatwick, GB(Pira International),* Session 4: 325, 327-339 (1997; Pira International).
14. Francis, P. E.; Lee, T. S; Use of Synthetic Environments for Corrosion Testing; *ASTM Special Tech. Publ. 970*: 300 p. (c1988).
15. Garner, A., Thompson, C. B.; Paper-Machine Corrosion and Progressive Closure of White-Water Systems Paprican (Pointe Claire: Québec: Canada). *1996 Papermakers Conference: Proceedings* Philadelphia,PA, 547-554 (March 24, 1996; TAPPI Press).
16. Garner, A., Thompson, C. B.; PAPER-MACHINE CORROSION AND PROGRESSIVE CLOSURE OF THE WHITE-WATER SYSTEM; *Proceedings [of*

the] 8th International Symposium and EFC[European Federation of Corrosion] on Corrosionin the Pulp & Paper Industry, Stockholm, Sweden, May 16-19, 1995, 207-216 (1995; Swedish Corrosion Institute).
17. Geller, A. N., Gottsching, L; Water System Closure in the Paper Industry; April 22-26, 1985; *NTRI (Pretoria) Symp. Forest Prods. Res. Int., Proc. Vol. 2,* Paper No. 5-4: 21 p. (April 22-26, 1985).
18. Geller, A.; Gottsching, L; Closing Water Systems Completely in the Federal Republic of Germany,*Tappi J.* 65, no. 9: 97-101 (Sept. 1982).
19. Gorelov, V. V.; Talybly, A. K; Corrosion Protection of Equipment in Closed and Reduced Water Recycling Systems; *Pulp & Paper Ind. Corrosion Problems/Proc. Int. Symp. Corrosion in Pulp & Paper Ind. (Stockholm)* 4th: 113-116 (May30-June 2, 1983).
20. Gudlauski, D. G.; EFFLUENT CLOSURE; WHITE-WATER SYSTEM CLOSURE MEANS MANAGING MICROBIOLOGICAL BUILDUP; Betz PaperChem Inc. (Jacksonville: FL:United States).; *Pulp & Paper* 70, no. 3: 161-162, 165 (March 1996).
21. Guest, D. A; Moore, G. K.; CLOSING UP OF WATER SYSTEMS: BENEFITS AND EFFECTS; Paper Technol. Ind. 23, no. 2: 65-70 (March 1982).
22. Hagen, Carl, Whitekettle, Kurt; COST-EFFECTIVE CONTROL METHODS DELIVER CONSISTENT WATER QUALITY; *Pulp & Paper* 72, no. 7: 75-76, 79-82.
23. Holy, A. V.; MICROBIOLOGICAL CORROSION; *Paper Southern Africa* 5, no. 5: 12, 16 (Sept./Oct. 1985.
24. Holy, A. von; Microbiologically Induced Corrosion - Are We on Target?; *Paper Southern Africa 8,* no. 2: 23, 26-27 (March 1988).
25. IDENTIFYING AND CONTROLLING PAPER MILL MICROBIOLOGICAL CORROSION; *Paper Trade J.* 156, no. 25: 46-8 (June 12, 1972).
26. Jong, R. L. de; NEW OXIDATIVE MICROBIOLOGICAL SYSTEM INVOLVING SULFATE-REDUCING BACTERIA AND COENZYME A; *Biotech 83 Proc. Int. Conf. Commercial Applns. Implications Biotechnol.* (London) 1st: 885-893 (c1983).
27. King, V. M.; Microbial Problems in Neutral/Alkaline Paper-Machine Systems; *TAPPI Environmental Anthology*: 298-303 (1991).
28. Knudsen, J. G; Somerscales, E. F. C.; FOULING OF HEAT TRANSFER EQUIPMENT; *Hemisphere Publ. Corp./McGraw-Hill (N.Y.)*: 743 p. (c1981).
29. Korhonen, J; Pursiainen, M.; Soimajarvi, J.; SULFATE-REDUCING BACTERIA IN PAPER MACHINE WATERS AND SUCTION-ROLL PERFORATIONS; *Appl. Microbiol. Biotechnol.* 5: 87-93 (1978).
30. Korhonen, J; Vestola, J.; CORROSION AND MICROBIOLOGICAL ACTION IN SUCTION ROLLS; *TAPPI Eng. Conf. (Toronto),* Preprinted Paper 17-1: 155-162 (Sept. 28-Oct. 2, 1975).
31. LaZonby, J.; DRAMATIC IMPROVEMENTS IN MICROBIOLOGICAL CONTROL USING THE SYNERGISTIC ACTIVITY BETWEEN SELECT ORGANIC BIOCIDES AND A NEW NONHALOGENATED OXIDANT; Nalco Chemicals.

32. Lott, L. F.; SECONDARY-FIBER PROCESSING DEPOSIT CONTROL; *15th International Conference on Pulping and Papermaking Technology*(Korea TAPPI): 3-11 (1991; Korea TAPPI).
33. Lott, L. F.; Secondary-Fiber-Processing Deposit Control; *J. TAPPIK* 24, no. 2: 44-52 (1992).
34. Lutey, R. W; MICROBIOLOGICAL DEPOSITS CONTROL; *TAPPI Papermakers Conf.* (Atlanta, Ga.): 133-44 (June 5-8, 1972).
35. Nathan, C. C.; Piluso, A. J; WET-END CORROSION PROBLEMS IN PAPER MILLS; NACE *Intern. Symp. Pulp Paper Ind. Corrosion Problems (Denver)* 2: 126-132 (May 1977); Paper Trade J. 161, no. 22: 32-35 (Nov. 15, 1977).
36. Piluso, A. J; CONTROLLING CORROSION IN PULP AND PAPER MILLS; Corrosion Inhibitors (C. C. Nathan, ed.): 236-239 (c1973 NACE).
37. Piluso, A. J; LOGICAL APPROACH TO WET-END PROBLEMS AND DEPOSIT CONTROL; *Southern Pulp Paper Mfr.* 40, no. 11: 14-18 (Nov. 1977).
38. PRATOMO, H.; REBAR CORROSION IN A CLARIFIER; Pabrik Kertas Tjiwi Kimia (Mojokerto: Indonesia).; *Proceedings [of the] 8th International Symposium and EFC [European Federation of Corrosion] Event No. 204 on Corrosion in the Pulp & Paper Industry,* Stockholm, Sweden, May 16-19, 284-288 (1995; Swedish Corrosion Institute).
39. Robertson, L. R.; Paper Chemistry; Clean Machine with Minimal Fresh Water;. *PIMA 77*, no. 4: 42-43 (April 1995).
40. Robertson, L. R.; Schwingel, W. R.; Effect of Water Reuse on Paper-Machine Microbiology; 1997 International Environmental Conference Minneapolis, MN, US. *(TAPPI, CPPA Technical Section, and USDA Forest Service):* 87-94 (May 4, 1997; TAPPIPress).
41. Robertson, L., Schwingel, W.; Microbial Challenges Unique to Closed Recycled Paper Systems; *Wet End Chemistry Conference Gatwick, GB(Pira International),* Session 4: 307, 309-324 (1997; Pira International).
42. Robertson, L.; Impact of Water Reuse on Paper-Machine Microorganisms; *1997 Biological Sciences Symposium: Proceedings* , San Francisco,CA US(TAPPI):145-154 (October 19, 1997; TAPPI Press).
43. Russell, P.; CORROSION CONTROL IN PAPER MACHINE WET-END ENVIRONMENTS; Weyerhaeuser Co; *TAPPI Adv. Topics Wet-End Chem. Sem.* (Atlanta) Notes: 117-127 (Oct. 23-25, 1985).
44. Safade, T. L.; Tackling the Slime Problem in a Paper Mill; *PIRA. (U.K.)*; *Paper Technol.* Ind. 29, no. 6: 280-285 (Sept. 1988).
45. Starnes, W. D; MICROBIOLOGICAL ANALYSES CAN AID IN SLIME CONTROL; *Pulp Paper* 47, no. 3: 94-7 (March, 1973).
46. T. E.; Gray, F; Microbiological Control in Paper Mills, *Cloete, Paper Southern Africa 5*, no. 4: 26, 28, 32 (July/Aug. 1985).
47. Tatnall, R. E; CASE HISTORIES: BACTERIA-INDUCED CORROSION; *Matls. Performance* 20, no. 8: 41-48 (Aug. 1981).
48. Thorpe, P. H; BACTERIAL CORROSION OF STAINLESS STEEL CAUSED BY WATERRECYCLING; *Corrosion Australasia* 4, no. 6: 12-14 (Dec. 1979).

49. Thorpe, P. H; MICROBIOLOGICAL CORROSION OF STAINLESS STEEL IN PAPER MACHINES AND ITS CAUSES; *Pulp & Paper Ind. Corrosion Problems/Int. Symp. Corrosion in Pulp & Paper Ind.* (Vancouver) 5th: 169-173 (June 3-6, 1986).
50. Thorpe, P. H; MICROBIOLOGICAL CORROSION OF STAINLESS STEEL IN PAPER MACHINES; *Appita 40*, no. 2: 108-111 (March 1987).
51. Tuthill, A. H.; BASE METAL RESISTANCE OF ALLOYS TO MICROBIOLOGICAL-INFLUENCED CORROSION; *Eng. Conf. (Boston) Proc. (Book 3)*: 975-984 (TAPPI; Sept. 14-17, 1992).
52. Van Orden, A. C.; Monitor On-Line Corrosion Electrochemically; *Chemical Engineering Progress 90*, no. 10: 67-73 (October 1994).
53. Wenzl, D. J. H; CLOSURE OF PAPER AND BOARD MILL PRODUCTION SYSTEMS AND ITS EFFECTS ON PRODUCTION CONDITIONS; *TAPPI Ann. Mtg. (Chicago) Proc.*: 95-109 (March 2-5, 1981).
54. Woodward, T. W.; WATER REUSE LEVELS, SOLIDS BUILDUP BARRIERS TO DEINKING-PLANT CLOSURE; *Pulp & Paper* 70, no. 2: 71-72, 75-76 (February 1996).
55. Woodward, T.; MILL CLOSURE: CRITICAL ISSUES; *PIMA* 78, no. 6: 44-45, 48-49 (June 1996).

Appendix I

ROLE OF THERMAL EXCURSIONS ON SULFIDATION OF CARBON STEEL

Safaa J. Al-Hassan, Gregory J. Fonder, and Preet M. Singh
Institute of Paper Science and Technology
500 Tenth St., NW
Atlanta, GA 30318
USA

ABSTRACT

The water wall tube surfaces in the lower furnace areas of kraft recovery boilers are exposed to a reduced sulfidizing atmosphere. Water wall surfaces are known to experience temperature excursions. High temperature excursions are relatively infrequent and most temperature spikes in this area are of small amplitude. Although it was known from the previous studies that continuous temperature cycling increases the corrosion rate of exposed metals, but the mechanism by which infrequent spikes increase the corrosion rate of carbon steel alloys in sulfidizing environment was not clear. The present study was aimed at establishing the effect of infrequent thermal excursions on overall high-temperature sulfidation of carbon steel used for water wall tubes. Results from the present study showed that even a couple of infrequent high-temperature thermal excursions, which can lead to scale damage, followed by long post spike exposure may lead to a higher corrosion rate than the equivalent isothermal tests conducted at the higher temperature of the thermal excursion.

INTRODUCTION

Thermal excursions are known to affect the corrosion behavior of metals in high-temperature gaseous environments. Most of the previously published work, studying the effects of thermal excursion on gaseous corrosion, was done with continuous thermal cycling for a given test period [1-4]. These studies clearly demonstrate that the corrosion attack is more severe due to the thermal cycling. A previous study [5] on SA-210 carbon steel alloy in a 1% H_2S environment at 320°C for 20 days reported that regularly spaced continuous spikes to 400°C increased the weight loss 19 times (compared with weight loss from 320°C isothermal test.) The same result represented a 374% increase when compared with weight loss from a 400°C isothermal test. In another study, 1.25Cr-0.5Mo steel in an oxidizing environment of 0.2% SO_2 with thermal cycling between high temperature and room temperature showed that corrosion rates

were strongly dependent on higher temperature; where the corrosion rates abruptly increased five folds around 700°C.[2]

Water wall tube surfaces in the lower furnace of the kraft recovery boilers, which have a reduced sulfidizing atmosphere, experience temperature excursions due to smelt/char layer spalling or other process disturbances. However, in the lower furnace of a kraft recovery boiler, high temperature thermal excursions are not very frequent. Most of temperature spikes at the lower furnace water wall surface of kraft recovery boiler are of small amplitude (~20°C), as shown in Figure 1. Temperature excursions, of 150°C or higher than normal operating temperature have been reported in floor tubes in the recovery boilers.[5] These excursions are very infrequent (a couple in four months of monitoring) and for relatively short time periods, typically between few minutes to few hours. For boilers operating between 300-350°C, upper temperature of excursions on the floor tubes was reported to be below 500°C.[6] High temperature excursions, with temperature changes of 100°C or more, can influence the corrosion of the boiler tubes on fireside by one or a combination of the following mechanisms:

- Increase in diffusion-controlled reaction rates and, therefore, overall sulfidation reaction rate,
- damage of semi-protective sulfide scale due to thermal stresses and thereby increase in reaction kinetics,
- changes in scale composition to an unprotective corrosion product, and
- molten salt corrosion (if the molten smelt is in contact with the fireside tube surface).

When the peak temperature is greater than the melting point of smelt then the molten salt corrosion will increase metal wastage significantly. However, the measured data indicate that peak temperature due to excursion does not exceed the melting point of smelt on inner wall tube surfaces in the lower furnace area.

Sulfidation rates are primarily determined by lattice diffusion in an undamaged sulfide scale. Diffusion in most common sulfides (FeS, Cr_2S_3, and NiS) is generally much faster than that in corresponding oxides due to higher concentration or mobility of defects in sulfide scales. [7] Damage of sulfide scale, due to thermal excursion, depends upon the thermal stresses generated in the scale, which in turn depends upon the relative coefficients of thermal expansion of the metal and the corrosion product scales. Other important factors in developing stresses in the scale are scale thickness and geometry of the metal surface. Stresses in the scale generally increase with an increase in scale thickness. Scales formed on curved surfaces have higher stresses than the scale formed on a flat surface. [8] For scales that grow at the scale/gas interface, the metal surface geometry will contribute to either compressive or tensile stresses depending on whether the curved surface is concave or convex. [9] Data on oxides show that NiO and CoO (with metal/oxide thermal expansion ratios of 1.03 and 0.93, respectively) seldom crack or spall on cooling to room temperature, while FeO and Cr_2O_3 (with 1.25 and 1.30 metal/oxide thermal expansion ratios, respectively) spall violently. [10] Stress buildup may be relieved through cracking of the scale or detachment of the scale from the parent metal.

The present study was aimed at establishing the role of infrequent thermal excursions on the corrosion of carbon steel water wall tubes from fireside. To do so, test parameters in the present work were changed so as to study the effects of scale damage and post-excursion exposure on the overall corrosion rate. Part of this study was presented at a symposium on corrosion in pulp and paper industry. [11]

EXPERIMENTAL WORK

SA-210 carbon steel specimens, 2.5 cm x 1.8 cm x 0.5 cm, were cut from a 5-cm-OD tube typical of that used in recovery boiler. Specimen preparation was carried out by burnishing the specimens in a drum with alumina triangles. A rust inhibiting additive and a detergent in distilled or deionized water were used in the burnishing process. [5] The chemical composition of SA-210 carbon steel alloy is given in Table 1. Specimens were cleaned with acetone and weighed before they were placed in the reaction tube.

A series of experiments were designed to study the effects of individual temperature excursions, at different time periods during the tests, on the corrosion rate of SA-210 carbon steel in a 1% H_2S environment. In these tests, coupons were exposed to a given set of conditions and were taken out at the end of each test to quantify corrosion measurements. These tests are referred to as "coupon tests" in this paper. Dimensions of thermal excursion are shown schematically in Figure 2. Tests were carried out for 72, 162, or 312 hours with temperature spikes at different times, as listed in Tables 2 through 4. A second set of experiments was carried out in thermobalance, using quartz spring, where the weight change was continuously monitored during any given test. These tests were referred to as "thermobalance tests."

All excursions took about 30 minutes to heat up, 30 minutes at 480°C, and then about 90 minutes to cool down to 320°C, as is shown schematically in Figure 2. The spike dimensions were kept constant throughout the present series of tests. Some isothermal tests were also carried out at 320°C and 480°C for different time periods to provide baseline data for comparison with the temperature excursion test data. Following cool down, the specimens were taken out of the reaction tubes, sulfide scale was removed from the surface of the specimen, and preserved for analysis by X-ray diffraction technique. Specimens were sandblasted to remove any attached scale, after which the specimens were weighed to an accuracy of 0.0001 g.

RESULTS AND DISCUSSION

Isothermal Tests

Tests were carried out for 4, 8, 24, 72, 162, and 312 hours at 320EC and 480EC to construct the baseline data with which the data from the thermal excursion tests could be compared. Results from the isothermal tests are shown in Figure 3. Weight loss from these tests shows that the weight loss increases as temperature and time increase. Results from 320EC isothermal tests plotted as log time vs. log weight loss indicate that the reaction follows a classical sulfidation behavior where initial corrosion rate and scale growth depend on reaction kinetics which is followed by a diffusion-controlled reaction occurring at a relatively lower rate. However, after certain limited time period (which decreases with an increase in temperature) the corrosion rates increase which may be due to sulfide scale cracking. Results from 480EC isothermal tests at any exposure time give higher corrosion rates compared to 320EC.

72-hour Tests

Coupon Tests A set of experiments was carried out at 320EC for 72 hours with only one temperature spike that was either at the beginning, the middle, or the end of these tests, as is shown schematically in Figure 4. Weight loss of SA-210 carbon steel was higher by 92%, 81%, and 39%, respectively, as compared to the weight loss from the isothermal test carried out at 320°C. However, the weight loss for these three tests was less than the isothermal test done at 480°C, where the weight loss was only 48%, 46%, and 34%, respectively, as is shown in Figure 5 and listed in Table 2.

These results can be explained by a simplistic model, which assumes that the temperature excursion only increases the instantaneous corrosion rate by increasing the diffusion and reaction kinetics. As is shown in Figure 6, the instantaneous corrosion rate $dC_{(Spike)}/dt_{(Spike)}$ for the spike time $dt_{(Spike)}$, is higher than the corresponding corrosion rate after the spike $dC_{(PS)}/dt_{(PS)}$ for post-spike time $dt_{(PS)}$. The corrosion rate, $dC_{(PS)}/dt_{(PS)}$, is similar to the corresponding 320°C isothermal corrosion rate at the same time period. The effect of spikes will be stronger in the beginning of scale growth and will diminish as the scale grows with time, as is shown schematically in Figure 6 and indicated by results in Figure 5.

Thermobalance Tests A series of tests were carried out where the weight change of the metal sample could be continuously monitored. This was done to quantify the effect of individual spikes in the 72-hour tests and to verify the model discussed in the previous section, as is shown schematically in Figure 6. Results from these tests are shown in Table 5. Results from the thermobalance tests were similar to the

results for coupon tests carried out under equivalent conditions. The effects of spike location were the same as those for the coupon tests. Weight loss of SA-210 carbon steel tested in the thermobalance was higher by 85% and 25% for the tests with spike at the beginning and the end of the of the tests, respectively, compared to the isothermal test carried out at 320°C. Equivalent numbers from the coupon tests were 92% and 39%, respectively. These results indicate that for short time periods, a simplistic model, like the one shown in Figure 6, can predict the role of infrequent spikes. This may be because a relatively thin sulfide scale does not get damaged by a thermal excursion. Therefore, the overall reaction is still controlled by the diffusion of reactants through the undamaged scale.

Double Spike Tests A series of experiments were conducted with double spikes at different times (as shown schematically in Figure 7) during the 72-hour tests to see if the effect of each spike is independent from the other one. Results from these tests show that the weight loss is higher for the tests with two spikes compared to corresponding spikes at single location, as is shown in Figure 8. The trend for the double spike tests was similar to the single spike tests, in the sense that, in general, the spikes in the beginning of the tests had a larger effect on the spikes at a later time. That shows that thermal excursion depends on the history of the scale as well as on the spike location. However, spike location seems to be the primary factor, since both tests associated with spike at the beginning, resulted in a higher weight loss compared to the tests carried out with spike at the end. Another test was carried out with thermal excursion in all three locations and results showed a 204% increase in weight loss compared to the isothermal test at 320°C. If we add the individual effect of each spike as shown in Figure 5 and Table 2, the total effect of spikes is a 208% increase in weight loss compared to the isothermal test at 320°C. This is very similar to the increase in weight loss (204%) for the test with spikes in three locations, as is shown in Figure 8. This indicates that for short exposure times, the effects of spikes are additive. Scale thickness for specimens tested for 72 hours may be less than the critical scale thickness required to develop stresses that cause scale damage.

Another experiment was conducted in which thermal excursions were continuous throughout the test period. This amounted to about 23 spikes in a 72-hour test and the weight loss was about 486% greater than the isothermal test at 320°C and about 150% greater than the isothermal test done at 480°C, as is shown in Figure 8. The results clearly show that continuous spikes may result in corrosion rates even higher than the isothermal tests carried out at the higher temperature (480°C). These results are consistent with previous work by Singbeil et al. [5], which reported that for coupons tested for 20 days at 320°C with regularly spaced spikes to 400°C increased the weight loss by 19 times when compared with results from 320°C isothermal tests.

162-hour Coupon Tests

Three experiments were carried out in which a single thermal excursion was introduced at three different locations (beginning, middle, or end) of the 162-hour test, as is shown in Table 3. The weight loss increases were 305%, 514%, and 25%, respectively, compared with isothermal tests carried out for 162 hours at 320°C. If we compare experiment 2 in Table 2 with experiment 12 in Table 3, both tests had a single spike, which starts after one hour of the beginning of the test. However, the test for 162 hours had a much longer post-spike exposure at 320°C than the 72-hour test. The effects of spike are much more significant for the 162-hour test (306% increase in weight loss compared to an equivalent 320°C isothermal test) compared to the 72-hour test (92% increase in weight loss compared to an equivalent 320°C isothermal test). Similarly, experiment 4 in Table 2 can be compared with experiment 13 in Table 3. Here the tests carried out for 162 hours had a 514% increase in weight loss compared to isothermal 320°C test; whereas, the test for 72 hours showed only 35% weight loss increase. This illustrates an important aspect of post-spike exposure. Experiment 14 in Table 3 was also a 162 hours test where there was almost no post-spike exposure, and the weight loss was close to the corresponding isothermal test at 320°C. If a spike leads to scale damage, then the effects will be clearly demonstrated in the post spike period by a significant increase in the corrosion rate.

312-hour Coupon Tests

A series of tests was carried out in which double spikes were conducted in a 312-hour test. The location of the double spikes is shown in Figure 9. Here the location of the second spike was fixed but the location of the first spike was varied from 24 hours to 168 hours. This was done to reduce the number of variables in two-spike systems in long duration tests. The first spike location was varied to see the effects of scale history on the resultant scale damage. However, we introduced a fixed 72-hr post-spike period after the second spike to see the combined effects of double spikes, as is shown in Figure 10. Results in Figure 10 and Table 4 show that the weight loss increased by 159%, 144%, and 229% for double spikes performed at the beginning, middle and end of the test, respectively, when compared to weight loss of the isothermal test at 320°C. It must be noted that the isothermal tests carried out at 320°C and 480°C for 312 hours have very high weight loss, as is shown in Figure 3 and Table 4. For the 320°C isothermal test, weight loss was about 4 times higher for the 312-hour test compared to the 162-hour test. The same results were 114%, 103%, and 165% higher corrosion rates for the tests with spikes at the beginning, middle, and end, respectively, when compared to weight loss of the isothermal test at 480°C, as is shown in Figure 10.

An important result from these experiments is that the weight loss for all 312-hour tests with only double thermal excursions was even higher than the isothermal tests carried out at 480°C. For short test times (up to 72 hours) the scale damage does not seem to participate in the overall sulfidation mechanism and a simplistic model based on diffusion and reaction kinetics, as shown schematically in Figure 6, can explain the effects of thermal excursion. However, in long duration tests, where thicker scales are more prone to scale damage due to thermal excursion, and the post-spike exposure effects become more predominant, the simplistic model does not explain these effects.

XRD of Sulfide Corrosion Products

If scale composition changes and the scale becomes unprotective, the corrosion rate may increase. To check this mechanism, sulfide scale was analyzed using powder X-ray diffraction technique. X-ray diffraction (XRD) of sulfide scale from coupon exposed at 480°C isothermal, 320°C isothermal, and test with continuous spiking reveals that chemical compositions of sulfide scale developed under these conditions are not very different. XRD patterns of sulfide scale from 480°C and 320°C isothermal tests indicate that FeS and $Fe_{1-x}S$ are the main phases of the corrosion products. Scale from continuous spiking shows similar pattern, as is shown in Figure 11. This suggests that the change in weight loss due to spiking to 480°C is not due to change in the chemical composition of the sulfide scale but may be due to scale damage.

Results from thermobalance study as well as coupon tests indicate that the damaged sulfide scales do not effectively heal in this system during post-spike exposure. These results have important implications for the kraft recovery boilers and other chemical processes that have a high-temperature sulfidizing atmosphere, in that, even a couple of infrequent spikes, followed by a long post-spike exposure, will lead to a very high corrosion rate. In the recovery boiler lower furnace, which experiences infrequent high-temperature spikes, even higher corrosion rates than the ones isothermally exposed at the higher temperature of spike may be experienced. In cases where the metal surfaces may undergo high-temperature thermal excursions, reducing the excursion amplitude and frequency will reduce the metal wastage significantly.

CONCLUSIONS

From our present results, it can be concluded that even a couple of infrequent spikes, which lead to scale damage, may lead to corrosion rates that are higher than the isothermal tests at higher temperature of the spike. For short duration tests (72 hours), in which sulfide scale is relatively thin, effects of thermal excursions depend upon change in diffusion-controlled reaction kinetics and can be easily explained by a simplistic model. However, in long duration tests, sulfide scales are thick and can get damaged due to thermal stresses developed by thermal excursions. The scale may not heal and protect

the exposed surface thereby leading to a higher corrosion rate in the post-spike exposure of metal. The scale damage depends upon amplitude and location of spike, scale composition, scale thickness, and history of exposure. In tested atmosphere and temperature range, sulfide scale composition does not change significantly on the carbon steel surface during thermal excursions. This leads us to conclude that the increase in metal wastage is primarily due to scale damage under these conditions.

ACKNOWLEDGMENTS

The authors would like to thank the DOE [Grant Number DE-FC36-95GO10092] and AF&PA for their financial support. The authors would like to thank the members of the AF&PA's Recovery Boiler Technical Advisory Group on Corrosion for their valuable suggestions and comments. The authors would also like to thank Mr. Douglas Singbeil of the Pulp and Paper Research Institute of Canada for providing the material, and Mr. Jamshad Mahmood of IPST for his help in specimen preparation.

REFERENCES

1. A. Hendry, *Corrosion Science*, 18, p.555 (1978).
2. A. C. Wong-Moreno, and A. B. Luisillo, *Oxidation of Metals*, 35 (3/4), p.245 (1991).
3. S. F. Chou, P. L. Daniel, A. J. Blazewicz, and R. F. Dudek, *High Temperature Corrosion in Energy Systems*, Editor; Michael F. Rothman, Warrendale, PA: Metallurgical Society of AIME, pp. 327-43 (1985).
4. D. Singbeil, L. Frederick, N. Stead, J. Colwell, and G. Fonder, *1996 TAPPI Engineering Conference Proceeding*, Vol. 2, TAPPI PRESS, Atlanta, p. 649 (1996).
5. James R. Keiser, et al, 9th International Symposium on Corrosion in the Pulp and Paper Industry, p.213, May 1998.
6. M. Mäkipää, S. Mäkinen, R. Backman, and M. Hämäläinen, *1996 TAPPI Engineering Conference Proceeding*, Vol. 2, TAPPI PRESS, Atlanta, p. 681 (1996).
7. S. Mrowec, and K. Przybylski, *High Temperature Materials and Processes*, 6(1&2): pp. 1-79 (1984).
8. K. Kofstad, "*High Temperature Corrosion*", London, Elsevier Ltd. Co., p. 249 (1988).
9. P. Hancock, and R.C. Hurst, in *Advances in Corrosion Science and Technology*, Vol. 4, R.W. Staehle, and M.G. Fontana, New York: Plenum Press, pp. 1-84 (1974).
10. R. F. Tylecote, *J. Iron Steel Inst.*, 196, p1232 (1960).
11. Safaa J. Al-Hassan, Gregory J. Fonder, and Preet M. Singh, 9th International Symposium on Corrosion in the Pulp and Paper Industry, p.255, May 1998.

TABLE 1
CHEMICAL COMPOSITION OF SA-210 CARBON STEEL ALLOY

Elements	C	Mn	Si	P	S	Fe
Weight %	0.21	0.65	0.22	0.01	0.016	Bal.

TABLE 2
SPIKE LOCATIONS DURING 72-HOUR TESTS

Experiment	Spike Location, Hr	Wt. Loss g/cm^2 $x10^4$ (mpy*)	%Wt Change w.r.t. 320°C	%Wt. Change w.r.t. 480°C
1-iso320	NA	11.6 (7)	----	----
2	1	22.2 (14)	192	49
3	34	21.0 (13)	181	46
4	69	15.6 (10)	135	34
5	1,34	27.8 (17)	240	61
6	1,69	30.8 (19)	266	68
7	34,69	21.9 (13)	189	48
8	1,34,69	35.2 (22)	304	78
9	Cont. Spikes	67.9 (41)	586	149
10-iso480	NA	45.6 (28)	----	----
(*) Calculations based on the assumption that the scale is a dense layer of FeS.				

w.r.t.: with respect to

TABLE 3
SPIKE LOCATIONS DURING 162-HOUR TESTS

Experiment	Spike Location, Hr	Wt. Loss, g/cm^2 $x10^4$ (mpy*)	%Wt Change w.r.t. 320°C	%Wt. Change w.r.t. 480°C
11-iso320	NA	14.2 (4)	----	----
12	1	57.7 (16)	406	----
13	80	87.2 (24)	614	----
14	159	17.7 (5)	125	----
15-iso480	NA	----	----	----
(*) Calculations based on the assumption that the scale is a dense layer of FeS.				

w.r.t.: with respect to

TABLE 4
SPIKE LOCATIONS DURING 312-HOUR TESTS

Experiment	Spike Location, Hr	Wt. Loss, g/cm^2 $x10^4$ (mpy*)	%Wt. Change w.r.t. 320°C	%Wt. Change w.r.t. 480°C
16-iso320	NA	56.7 (8)	----	----
17	24,267	89.9 (13)	159	114
18	96,267	81.6 (12)	144	103
19	168,267	130 (18)	229	165
20-iso480	NA	78.9 (11)	----	----
(*) Calculations based on the assumption that the scale is a dense layer of FeS.				

TABLE 5
SINGLE SPIKE EFFECT FROM THERMOBALANCE AND COUPON EXPERIMENTS DURING 72-HOUR TESTS

Tests	Spike Location, Hr	Coupon		Thermobalance	
		%Wt Change w.r.t. 320°C	%Wt. Change w.r.t. 480°C	%Wt Change w.r.t. 320°C	%Wt. Change w.r.t. 480°C
single	1	192	49	185	43
single	34	181	46	160	37
single	69	135	34	125	29

w.r.t.: with respect to

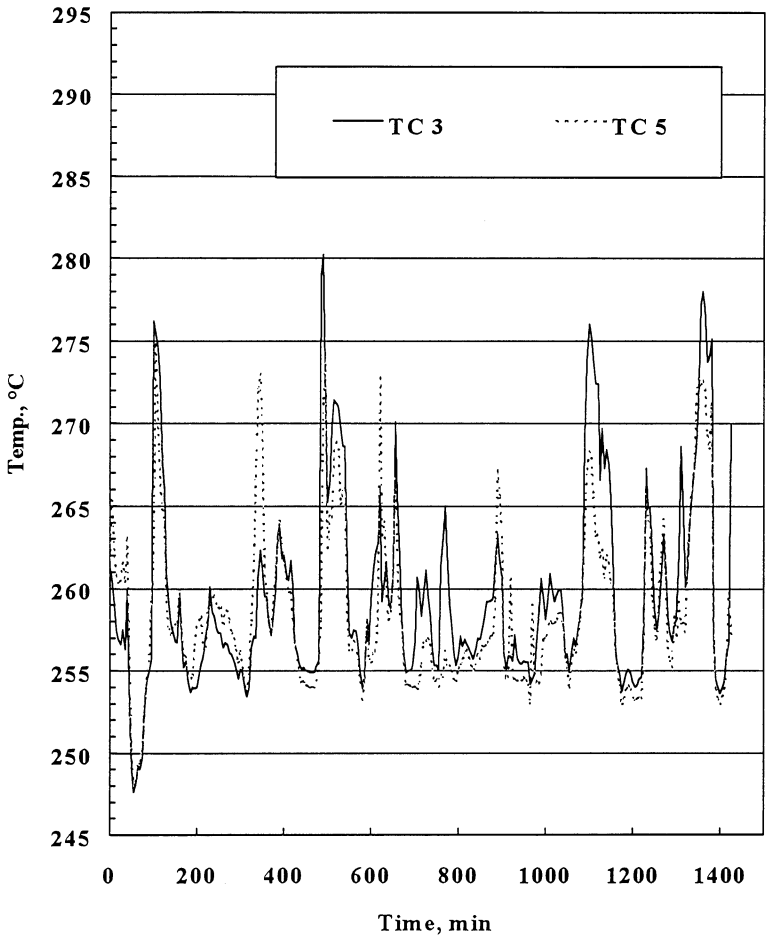

FIGURE 1. **Water wall temperature profile from lower furnace of kraft recovery boiler using two membrane-imbedded thermocouples.**

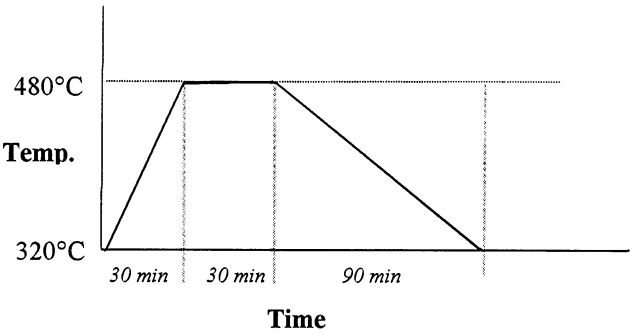

FIGURE 2. **Schematic diagram showing the dimensions of an individual thermal excursion carried out during the present work.**

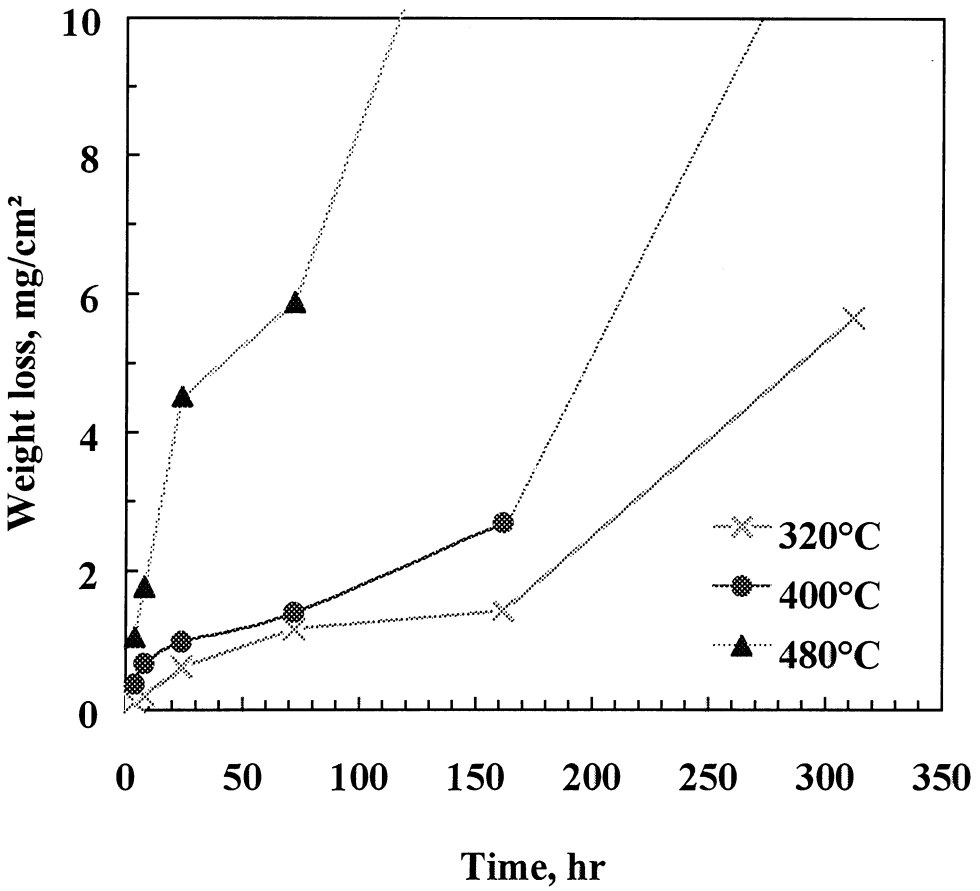

FIGURE 3. **Weight loss for SA-210 carbon steel alloy in 1% H_2S environment at 320°C and 480°C.**

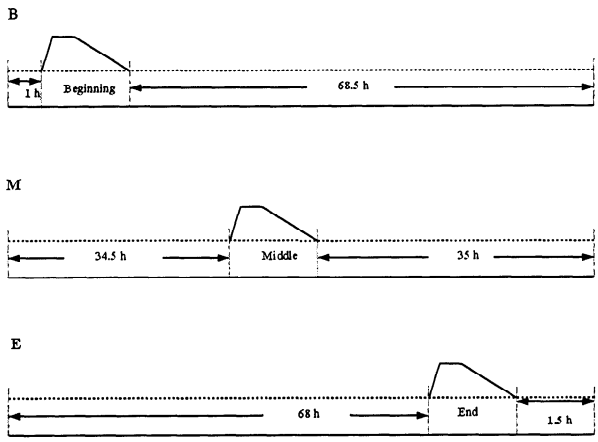

FIGURE 4. **Schematic diagram showing the single spike locations during 72-hour tests in 1% H_2S environment.**

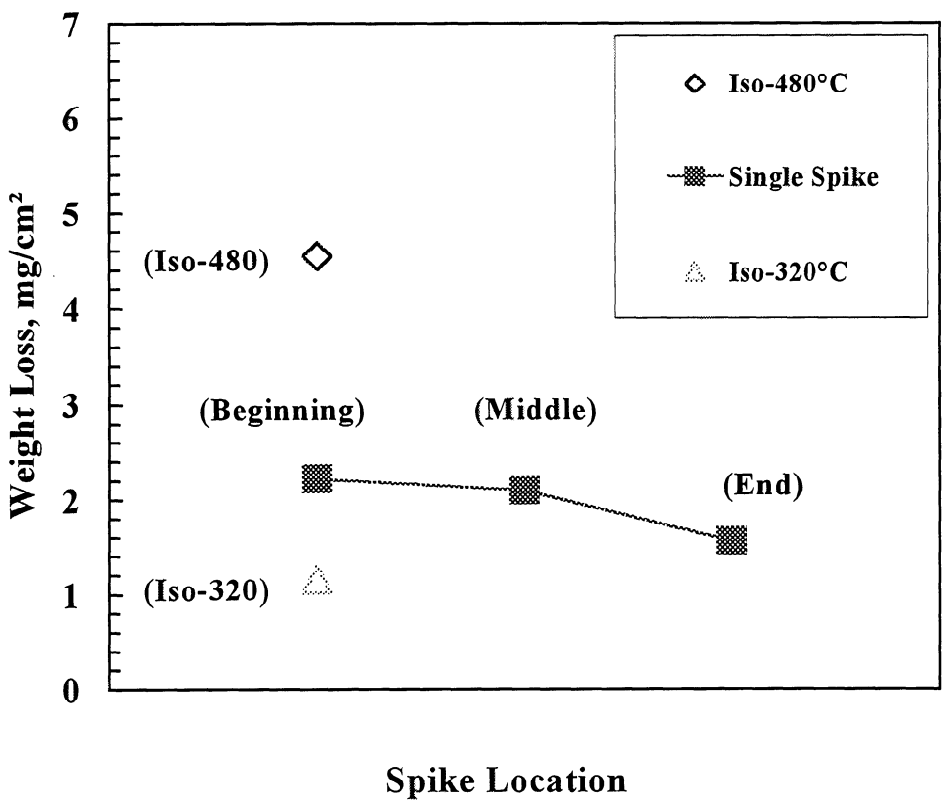

FIGURE 5. **Weight loss as a function of single thermal excursion carried out during 72-hour tests of SA-210 carbon steel alloy in 1% H_2S environment.**

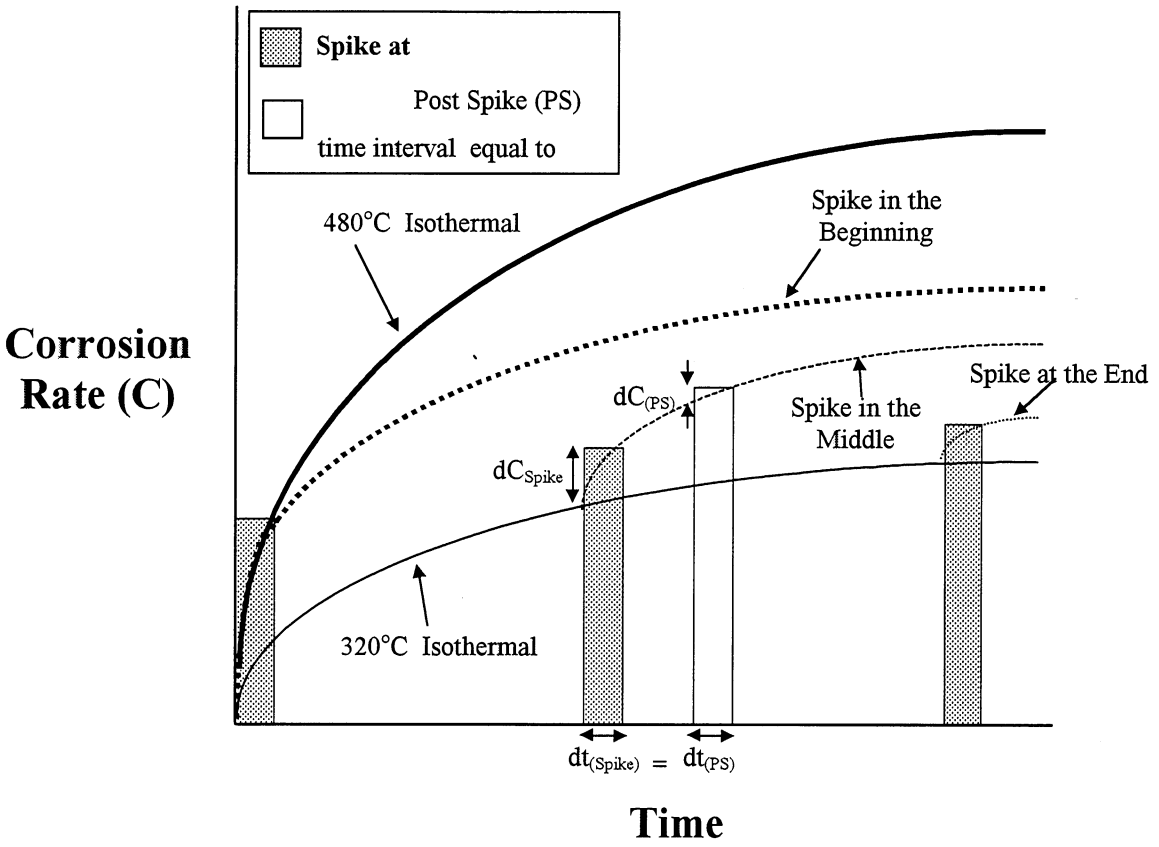

FIGURE 6. **Simplistic showing the effect of spike location on sulfidation rate.**

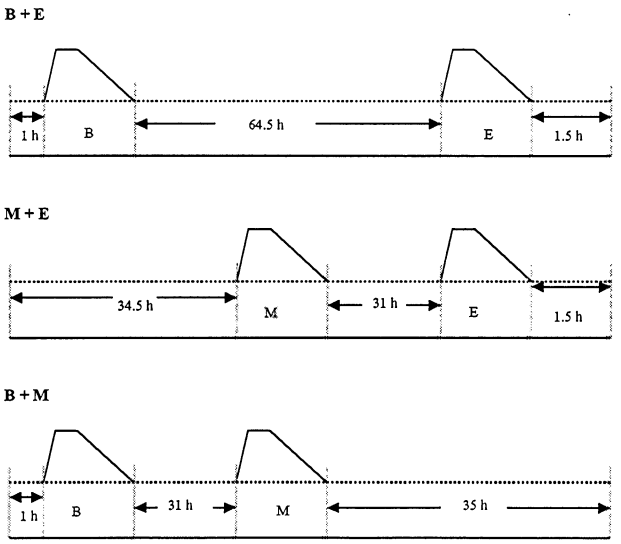

FIGURE 7. **Schematic diagram showing the double spike locations during 72-hour tests in 1% H_2S environment, where B, M, or E, is spike location at the beginning, middle, or at the end, respectively.**

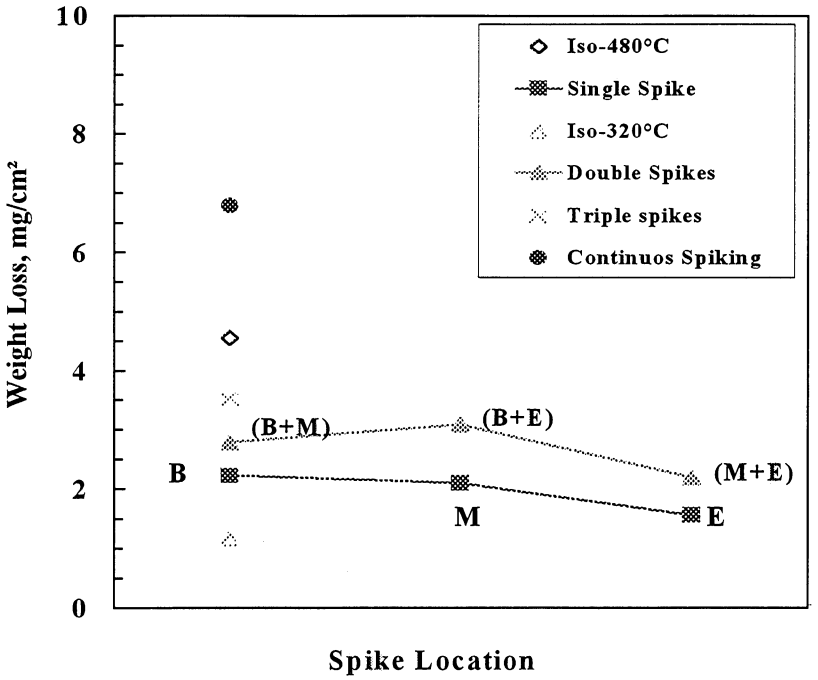

FIGURE 8. Weight loss for SA-210 specimens as a function of double spike location for 72-hour tests in 1% H_2S environment, where B, M, or E, is spike location at the beginning, middle, or at the end, respectively.

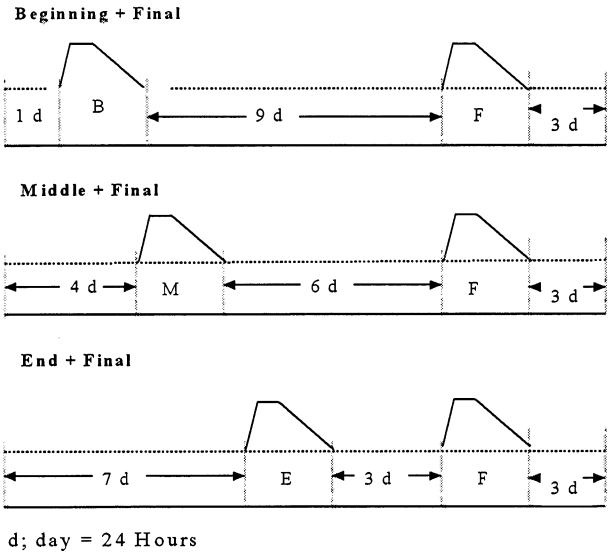

FIGURE 9. Schematic diagram showing the double spike locations during 312-hour tests in 1% H_2S environment, where B, M, E, or F is spike location at the beginning, middle, end, or at the final location, respectively.

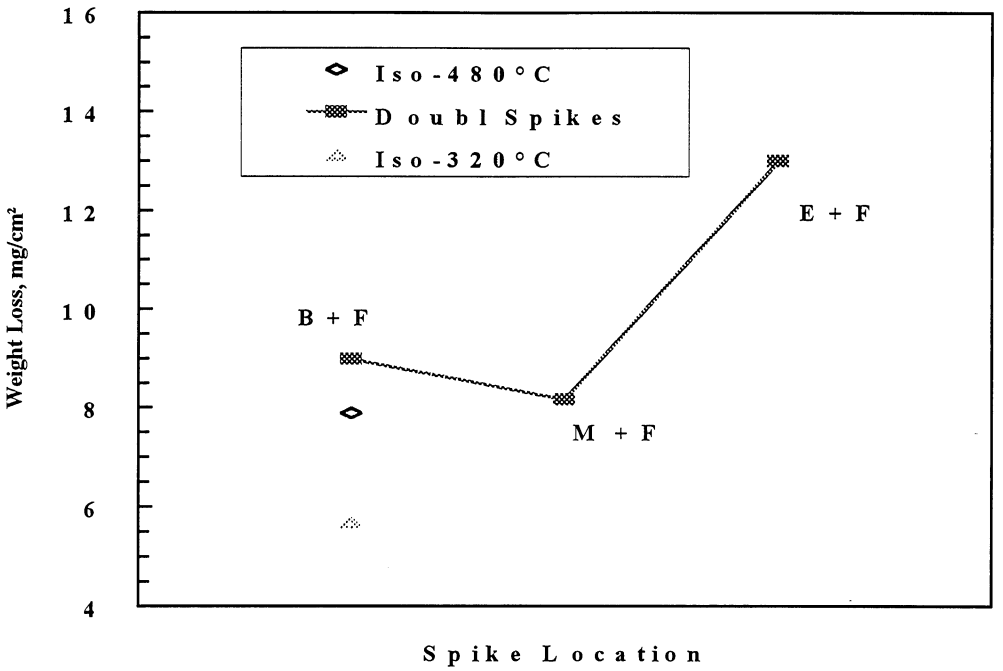

FIGURE 10. **Weight loss of SA-210 specimens due to double thermal excursions carried out during 312-hour tests in 1% H_2S environment, with spike location as in Figure 9.**

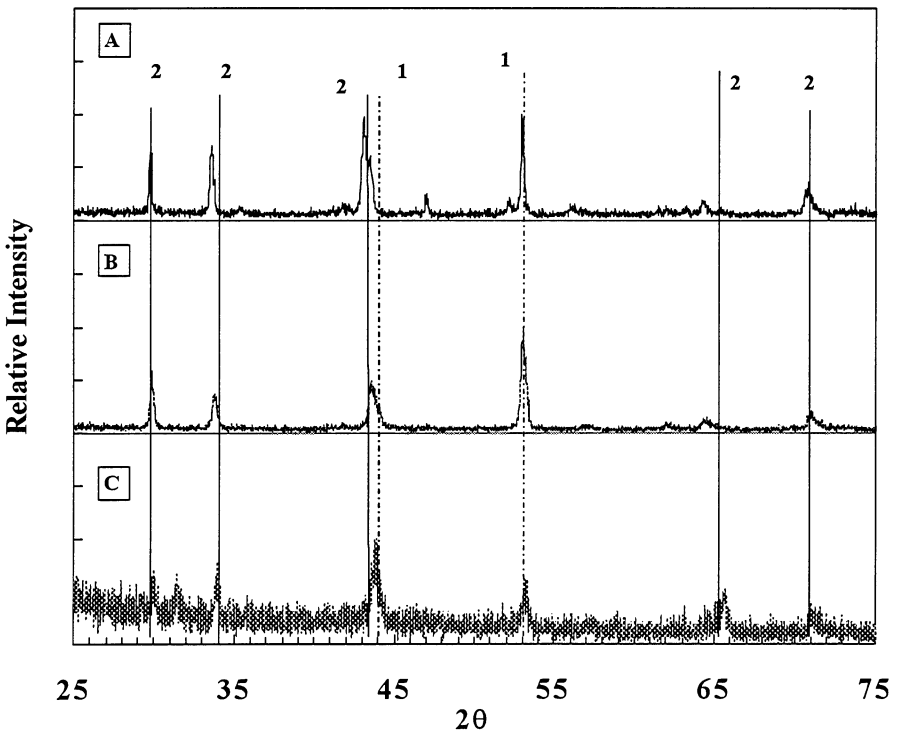

FIGURE 11. **XRD pattern for scale from Iso-480°C (A), Iso-320°C (B), and Continuous Spiking (C), all for 72-hours. Phase 1 represents iron sulfide (FeS); phase 2 represents iron sulfide ($Fe_{1-x}S$).**

Appendix II
Chemical analysis of white waters after different time periods

Table A1 ICP results showing corrosion products in different solutions after exposure of test coupons for 2 and 7 days

Project:	**F019**
Receipt Date:	**2/15/1999**
Client:	**IPST**
IPST Contact:	**Preet Singh**

Lab ID:	Client ID:	Fe	Ni	Cr	Mo
		(mg/L)	(mg/L)	(mg/L)	(mg/L)
35-99-072-1 Fresh	Baseline, pH=4.0,T 02	0.003	< 0.013	< 0.007	< 0.016
35-99-072-2 Fresh	Baseline, pH=9.0,T 02	0.009	< 0.013	< 0.007	< 0.002
35-99-072-3 Fresh	Strong, pH=4.0,T 02	0.030	< 0.131	< 0.071	< 0.163
35-99-072-4 Fresh	Strong, pH=9.0,T 02	< 0.027	< 0.131	< 0.071	< 0.163
35-99-072-5 Exposed 3 days	Baseline, pH=4.0,T 12	0.008	0.061	< 0.007	< 0.016
35-99-072-6 Exposed 3 days	Baseline, pH=9.0,T 12	0.003	< 0.013	< 0.007	< 0.016
35-99-072-7 Exposed 3 days	Strong, pH=4.0,T 12	1.16	< 0.131	< 0.071	< 0.163
35-99-072-8 Exposed 3 days	Strong, pH=9.0,T 12	< 0.027	< 0.131	< 0.071	< 0.163

Table A2 Chemical analysis of white water after different time periods

Project:	F019			
Client:	IPST			
Contact:	P.Singh			
Lab ID:	35-99-065			
		Results (mg/L)		
Sample	Rep.	Chloride	Sulfate	Thiosulfate
Fresh Solutions				
T0 Tappi 4	1			
T0 Tappi 4	2	167	425	38
T0 Tappi 4	3	169	437	39
T0 Tappi 9	1	167	428	39
T0 Tappi 9	2	170	439	37
T0 Tappi 9	3	168	434	38
T0 Strong 4	1	1679	4352	401
T0 Strong 4	2	1706	4415	391
T0 Strong 4	3	1658	4281	388
T0 Strong 9	1	1706	4525	388
T0 Strong 9	2	1692	4451	408
T0 Strong 9	3	1659	4353	378
After one day (Coupons were exposed to these solutions)				
T1 Tappi 4	1	176	457	41
T1 Tappi 4	2	173	441	40
T1 Tappi 4	3	171	435	37
T1 Tappi 9	1	170	451	40
T1 Tappi 9	2	173	455	41
T1 Tappi 9	3	171	441	39
T1 Strong 4	1	1720	4610	410
T1 Strong 4	2	1735	4633	399
T1 Strong 4	3	1715	4389	381
T1 Strong 9	1	1739	4613	407
T1 Strong 9	2	1765	4574	417
T1 Strong 9	3	1756	4520	392
Fresh Solutions				
T00 Tappi 4	1	208	525	46
T00 Tappi 4	2	215	534	48
T00 Tappi 4	3	212	529	46
T00 Tappi 9	1	211	533	48
T00 Tappi 9	2	209	524	48
T00 Tappi 9	3	208	523	47
T00 Strong 4	1	2083	5303	497
T00 Strong 4	2	2066	5229	481
T00 Strong 4	3	2357	5392	505
T00 Strong 9	1	2083	5255	485
T00 Strong 9	2	2076	5448	471
T00 Strong 9	3	2116	5223	483

After three days (Kept in Bath but without Coupons)				
T02 BL 4	1	211	507	46
T02 BL 4	2	209	511	44
T02 BL 4	3	220	536	47
T02 BL 9	1	206	510	45
T02 BL 9	2	208	517	42
T02 BL 9	3	210	520	44
T02 Strong 4	1	2147	5303	505
T02 Strong 4	2	2201	5363	487
T02 Strong 4	3	2125	5238	497
T02 Strong 9	1	2142	5250	502
T02 Strong 9	2	2117	5225	469
T02 Strong 9	3	2205	5437	508
Solution after 3 days (coupons exposed in these Solns.)				
T12 BL 4	1	207	507	40
T12 BL 4	2	211	512	40
T12 BL 4	3	211	516	42
T12 BL 9	1	199	501	43
T12 BL 9	2	222	541	48
T12 BL 9	3	210	523	48
T12 Strong 4	1	2062	5163	461
T12 Strong 4	2	2254	5518	505
T12 Strong 4	3	2164	5290	485
T12 Strong 9	1	2017	5046	468
T12 Strong 9	2	2277	5587	523
T12 Strong 9	3	2183	5388	505
Solution after 7 days (Kept in bath but without coupons)				
T03 BL 4	1	204	521	44
T03 BL 4	2	206	506	44
T03 BL 9	1	199	516	44
T03 BL 9	2	197	510	42
T03 Strong 4	1	1991	5082	474
T03 Strong 4	2	2015	5149	484
T03 Strong 9	1	2020	5126	472
T03 Strong 9	2	2031	5117	475
Solution after 7 days (coupons exposed in these Sols.) t = solution from top; b = solution from Bottom				
T13t BL 4	1	206	517	41
T13t BL 4	2	205	518	42
T13t BL 9	1	203	513	46
T13t BL 9	2	201	512	46
T13t Strong 4	1	2027	5046	460
T13t Strong 4	2	2033	5105	468
T13t Strong 9	1	2075	5228	485
T13t Strong 9	2	2101	5334	491
T13b BL 4	1	217	545	43
T13b BL 4	2	215	548	43
T13b BL 9	1	213	543	49
T13b BL 9	2	214	549	49
T13b Strong 4	1	2120	5429	478

T13b Strong 4	2	2158	5486	488
T13b Strong 9	1	2135	5557	508
T13b Strong 9	2	2165	5613	511